Higgs Physics
Experimental Overview

PHENOEXP Workshop

August 10 – 12, 2026

São Paulo, Brazil

ICTP-SAIFR/IFT-UNESP

Marisilvia Donadelli
Universidade do Estado do Rio de Janeiro

Disclaimer: based on many of the excellent talks given at ICHEP 2026

Rich Physics Measurement Program with Excellent Accelerator and Detector Performance

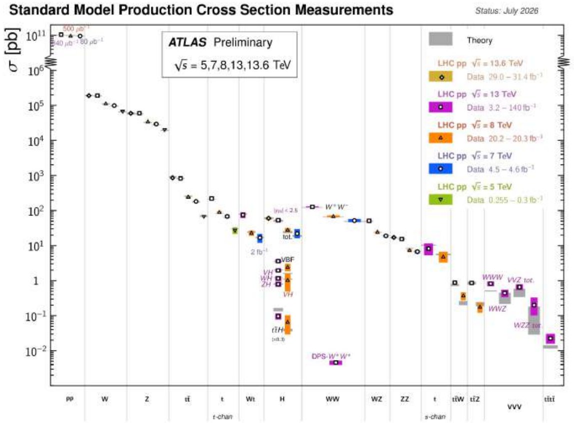

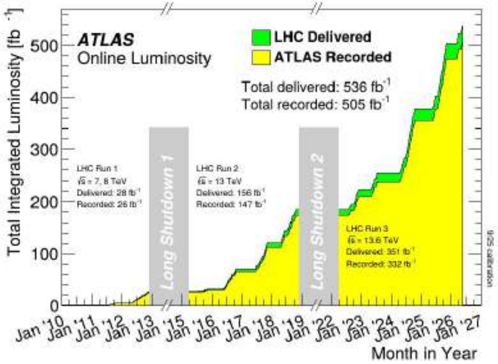

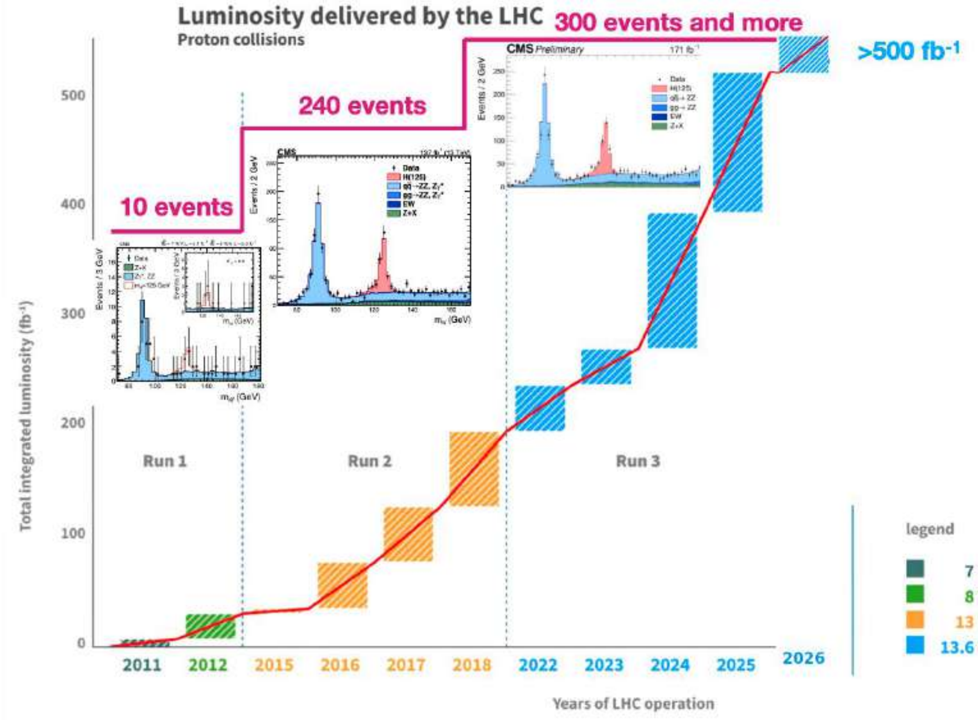

Summary of SM cross-section measurements

- SM Higgs production cross-sections at $\sqrt{s}$ = 7, 8, and 13 TeV, corrected for branching ratios and compared to theoretical predictions (LO QCD if not specified).
- Fiducial region: $\sqrt{s}$ = 13 TeV results are shown for $|y_H| < 2.5$, combining production modes and decay channels from original analyses.

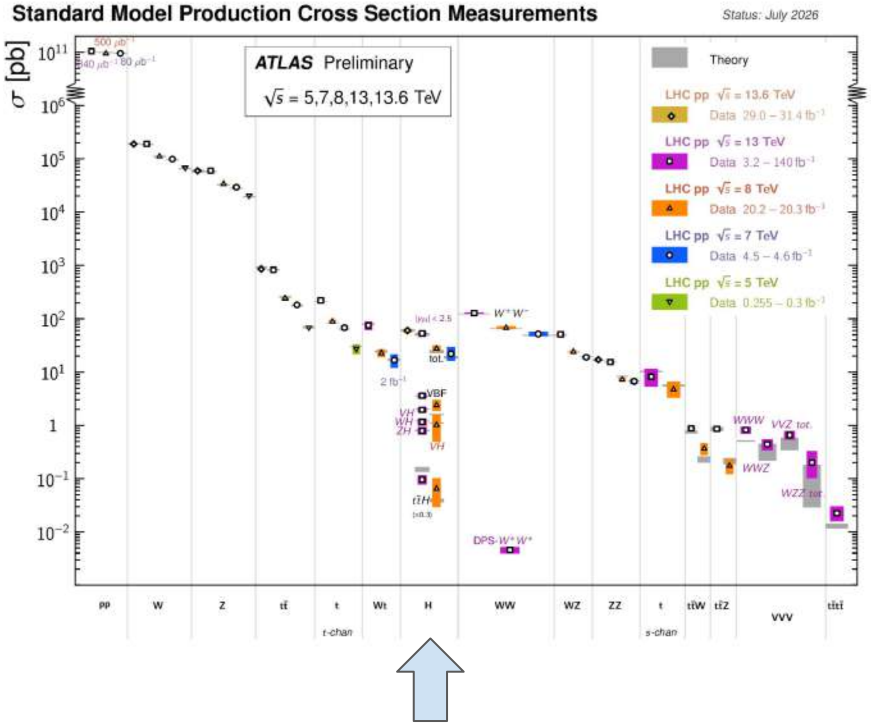

Combination of Higgs boson measurements at $\sqrt{s}$ = 13 TeV

More than 10 years after the discovery of the Higgs boson, we continue to improve the precision of its property measurements.

CERN-EP-2026-228 (to appear)

- Precision Higgs measurements are now a key test of the Standard Model and a probe for BSM physics.
- Run 2 provides over 30 times more recorded Higgs bosons than the Run 1 discovery dataset.
- This combination exploits all available channels simultaneously to provide the most comprehensive picture of Higgs boson interactions.

Phys.Lett. B716 (2012) 1-29

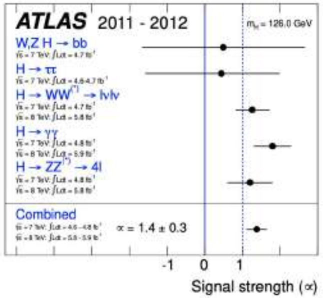

Nature 607, 52-59 (2022)


Article | Open access | Published: 04 July 2022

A detailed map of Higgs boson interactions by the ATLAS experiment ten years after the discovery

The ATLAS Collaboration

Nature 607, 52–59 (2022) | Cite this article

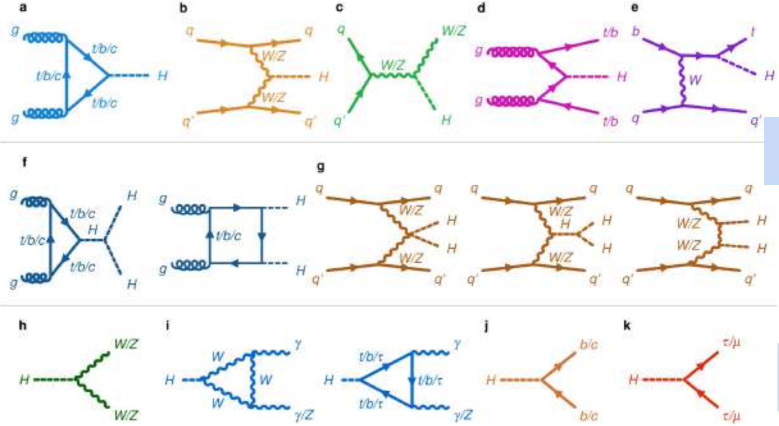

production

decay

Input analyses - CMS

- Integrated luminosity : 138 fb^{-1}
- Combined fit spans up to 1951 event categories
- Over 10^4 fit parameters cover parameters of interest plus experimental and theoretical systematic uncertainties

Input analysis	Decay channels targeted	Production targeted	Signal granularity	References
$H \to \gamma\gamma$	$\gamma\gamma$	ggH, (N_J, p_T^H, m_{jj}) bins VBF, (p_T^H, m_{jj}, p_T^{Hjj}) bins VH hadronic WH leptonic, p_T^V bins ZH leptonic ttH, p_T^H bins tH	STXS stage 1.2	[42]
$H \to ZZ \to 4\ell$	4μ, $2e2\mu$, $4e$	ggH, (N_J, p_T^H, m_{jj}) bins VBF, (N_J, p_T^H, m_{jj}, p_T^{Hjj}) bins VH hadronic VH leptonic, p_T^V bins ttH	STXS stage 1.2	[43]
$H \to WW \to \ell\nu\ell\nu$	$e\mu/\mu e$, ee+$\mu\mu$, $e\mu$+jj 3ℓ, 4ℓ	ggH, (N_J, p_T^H) bins VBF-like (p_T^H, m_{jj}) bins VH hadronic WH leptonic, p_T^V bins ZH leptonic, p_T^V bins	STXS stage 1.2	[44]
$H \to \tau\tau$	$e\mu$, $e\tau_h$, $\mu\tau_h$, $\tau_h\tau_h$ $e\tau_h$+2ℓ, $\mu\tau_h$+$\ell/2\ell$, $\tau_h\tau_h$+$\ell/2\ell$	ggH, (N_J, p_T^H, m_{jj}) bins VBF, (N_J, p_T^H, m_{jj}) bins WH leptonic, p_T^V bins ZH leptonic, p_T^V bins	Inclusive production processes or STXS stage 1.2	[45]
$H \to bb$ boosted	bb	ggH, high-p_T^H bins VBF, high-p_T^H bins	Inclusive production processes or STXS stage 1.2	[27]
VBF ($H \to bb$)	bb	VBF	Inclusive production processes	[26]
VH ($H \to bb$)	bb	WH leptonic, p_T^V bins ZH leptonic, p_T^V bins	STXS stage 1.2	[30]
t(t)H ($H \to bb$)	bb	ttH, p_T^H bins tH	Inclusive production processes or STXS stage 1.2	[31]
t(t)H ($H \to$ leptons)	2ℓ(same charge), 3ℓ, 4ℓ 1ℓ+$2\tau_h$, 2ℓ(same charge)+$1\tau_h$, 3ℓ+$1\tau_h$	ttH, tH	STXS stage 1.2	[46]
$H \to \mu\mu$	$\mu\mu$	ggH, VBF, VH, ttH	Inclusive production processes	[47]
$H \to Z\gamma \to \ell\ell\gamma$	$\ell\ell\gamma$	ggH, VBF	Inclusive production processes	[48]
$H \to$ inv	Large p_T^{miss}	Monojet VBF VH leptonic VH/ttH hadronic	Inclusive production processes	[29, 49–51]
Off-shell ($H \to ZZ \to 4\ell$)	4ℓ	Off-shell	Off-shell contributions (cf. Eq. (17))	[28]

CMS-HIG-21-018

Input analyses - ATLAS

Compared to the Nature combination, this analysis benefits from more data in several channels, improved analysis techniques, and the inclusion of new channels.

- Integrated luminosity : 126-140 fb^{-1}
- 14 on-shell analyses
  - 6 unchanged
  - 8 updated or new
- 4 $\boldsymbol{H} \rightarrow$ inv analyses
- 2 off-shell analyses
- 6 di-Higgs analyses
- Systematic uncertainties:
  - Correlated for consistent definitions/calibration/modelling schemes across analyses
  - $\approx$ 600– 800 analysis regions
  - $\approx$ 6000– 8000 nuisance parameters

CERN-EP-2026-228
(to appear)

Analysis	Prod. modes	$\mathcal{L}$ [fb^{-1}]	Ref.	Comparison with Ref. [3]	Measurements Incl.	κ	STXS
$H \rightarrow ZZ^* \rightarrow 4\ell$	All	140	[73]	Unchanged	✓	✓	✓
$H \rightarrow WW^* \rightarrow \ell\nu\ell\nu$	ggF, VBF	140	[74]	Updated	✓	✓	✓
$H \rightarrow WW^* \rightarrow \ell\nu\ell\nu, \ell\nu jj$	VH	140	[75]	Full Run 2	✓	✓	✓
$H \rightarrow \gamma\gamma$	All	140	[76]	Unchanged	✓	✓	✓
$H \rightarrow Z\gamma$	All	140	[70]	Unchanged	✓	✓	
$H \rightarrow \tau\tau$	All, except $(V \rightarrow \text{leptons})H$	140	[77]	Updated	✓	✓	✓
$H \rightarrow \tau\tau$	$(V \rightarrow \text{leptons})H$	140	[72]	New	✓	✓	
$H \rightarrow \mu\mu$	All	140	[71]	Unchanged	✓	✓	
$H \rightarrow bb$	VBF	126	[5]	Unchanged	✓	✓	✓
$H \rightarrow bb, cc$	$(V \rightarrow \text{leptons})H$	140	[78]	Updated	✓	✓	✓
$H \rightarrow bb$ (high p_T^H)	All	136	[69]	Unchanged			✓
$H \rightarrow$ multileptons	ttH	140	[79]	Full Run 2	✓	✓	✓
$H \rightarrow bb$	ttH	140	[80]	Updated	✓	✓	✓
$H \rightarrow bb$	tH	140	[81]	Updated	✓	✓	✓
$H \rightarrow$ invisible	VBF	140	[65]	Unchanged		✓	
$H \rightarrow$ invisible	VBF + γ	140	[68]	New		✓	
$H \rightarrow$ invisible	$(V \rightarrow \text{leptons})H$	140	[66]	Unchanged		✓	
$H \rightarrow$ invisible	ttH	140	[67]	New		✓	
$H^{(*)} \rightarrow ZZ^{(*)}$	ggF, VBF	140	[63]	Updated		✓	
$H^{(*)} \rightarrow WW^{(*)}$	ggF, VBF	140	[64]	New		✓	
$HH \rightarrow bbbb$	ggF, VBF	126	[6]	New		✓	
$HH \rightarrow bbbb$ (high p_T^H)	VBF	140	[82]	New		✓	
$HH \rightarrow bb\tau\tau$	ggF, VBF	140	[83]	New		✓	
$HH \rightarrow bb\gamma\gamma$	ggF, VBF	140	[84]	New		✓	
$HH \rightarrow bb\ell\ell + E_T^{\text{miss}}$	ggF, VBF	140	[85]	New		✓	
$HH \rightarrow$ multileptons	ggF, VBF	140	[86]	New		✓	

Global signal strength - ATLAS

- Inclusive Higgs production and decay rate: total uncertainty improved by ~15% vs. the Nature publication

- The SM compatibility quantified by p_{SM} value, derived using the asymptotic χ^2 distribution

$$p_{\text{SM}} = 1 - F_{\chi^2_n}(q(\vec{a}_{\text{SM}}))$$

CERN-EP-2026-228 (to appear)

- SM compatibility p_{SM} = 77%

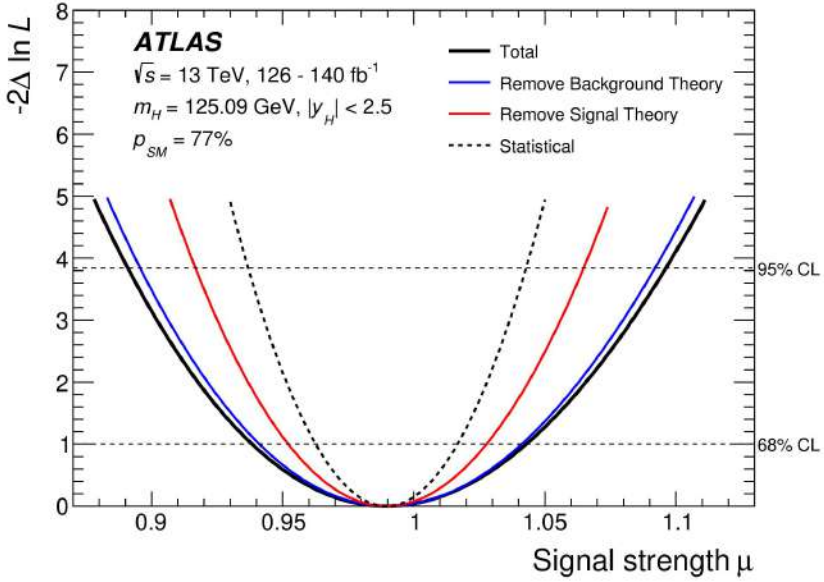

signal-theory uncertainty: dominant contribution to the total uncertainty

- QCD: $^{+0.026}_{-0.024}$
- PS/UE: $^{+0.019}_{-0.018}$
- PDF: $^{+0.017}_{-0.015}$

$$\mu := \frac{\sigma_i \cdot \mathcal{B}^f}{(\sigma_i \cdot \mathcal{B}^f)_{\text{SM}}} = \frac{\text{observed rate}}{\text{expected rate}} = 0.990^{+0.053}_{-0.051} = 0.990 \pm 0.027\,(\text{stat.}) \pm 0.024\,(\text{exp.})\, ^{+0.037}_{-0.035}\,(\text{sig. theo.})\, ^{+0.016}_{-0.015}\,(\text{bkg. theo.})$$

Production cross-section and BR measurements

- Production cross sections measured across 6 modes (ggF+bbH, VBF, WH, ZH, ttH, tH), with BRs fixed to SM values
- Up to 45% tighter total uncertainties vs. the Nature combination;
- SM compatibility p_{SM} = 20%

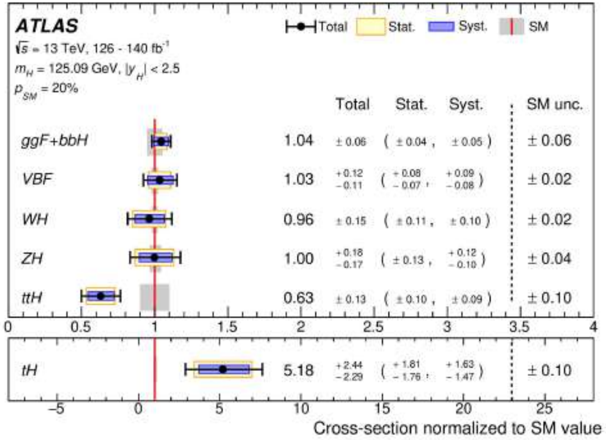

CERN-EP-2026-228 (to appear)

- BR measurements (production cross sections fixed to SM): γγ/ZZ/WW decays ~10% total uncertainty; bb/ττ ~10%
- μμ/cc and Zγ decays: >50% uncertainty, still statistics-dominated — expect large gains with more data
- SM compatibility: p_{SM} = 85%

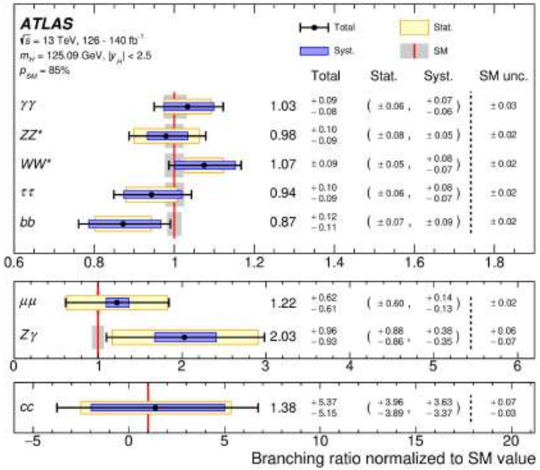

m_b (m_H) interpretation

The $H \to bb$ probes the bottom Yukawa coupling and, through it, the running b-quark mass

Methodology: the ratio Γ_{bb}/Γ_{ZZ} is measured and reparameterized as a function of m_b m_H using high-order QCD and electroweak calculations (N4LO (QCD) + NLO (EW) in HDECAY 6.61)

$$\frac{(\Gamma_{bb}/\Gamma_{ZZ})_{\text{obs}}}{(\Gamma_{bb}/\Gamma_{ZZ})_{\text{SM}}} = 0.96^{+0.20}_{-0.17}$$

$$\frac{\Gamma_{bb}}{\Gamma_{ZZ}} = \left(\frac{\Gamma_{bb}}{\Gamma_{ZZ}}\right)_{\text{SM}} \left(1 + \sum_{n=1}^{5} a_n \left[\left(\frac{m_b(m_H)}{m_b^{\text{ref}}}\right)^n - 1\right]\right)$$

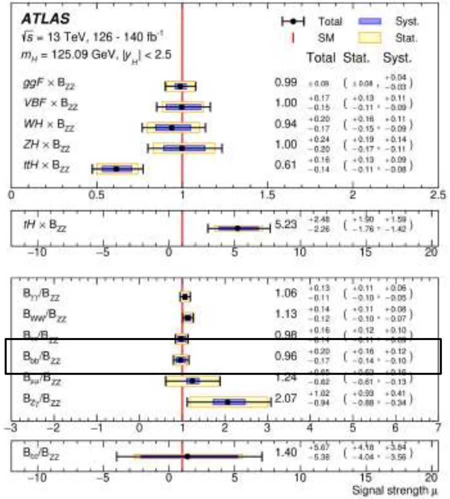

CERN-EP-2026-228
(to appear)

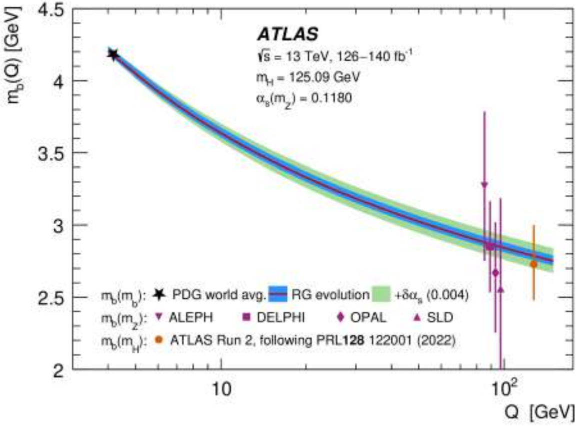

This provides the first ATLAS direct determination of m_b (m_H) in a combined Higgs coupling fit

Reject the no-running hypothesis by more than 8 sigma

$$m_b(m_H) = 2.73^{+0.27}_{-0.25}\ \text{GeV} = 2.73^{+0.22}_{-0.20}(\text{stat.})^{+0.15}_{-0.14}\ (\text{syst.})^{+0.07}_{-0.06}\ (\text{theo.})\ \text{GeV}$$

Simplified Template Cross-Section (STXS) measurement

- Production phase space split into 44 kinematic regions (8 more than the Nature combination), assuming SM-like Higgs BRs — sharpens sensitivity to BSM effects while limiting theory uncertainty and model-dependence from acceptance extrapolation
- Up to ~35% improvement in precision
- SM compatibility $p_{\mathrm{SM}} = 47\%$

CERN-EP-2026-228
(to appear)

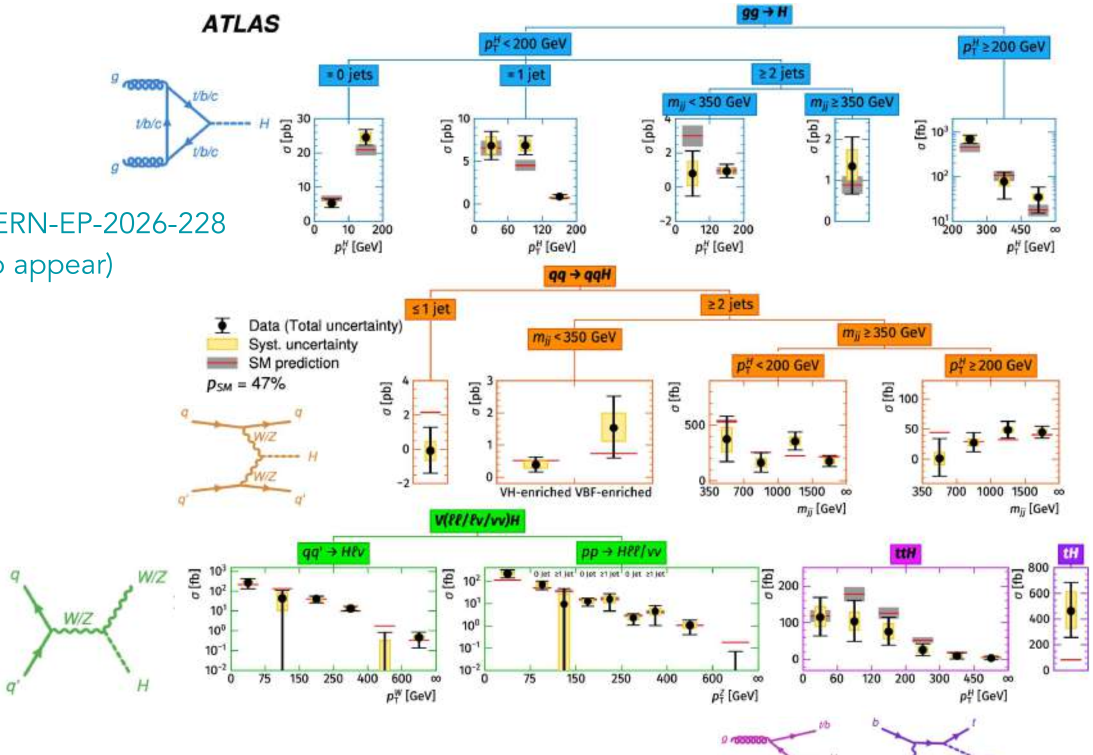

CERN-EP-2026-228

Simplified Template Cross-Section (STXS) measurement

- Production phase space divided into 32 kinematic regions
- Merged some bins to avoid large uncertainties or large correlations

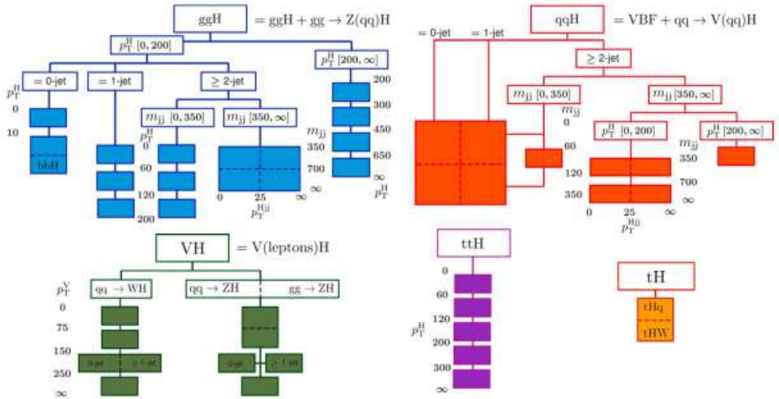

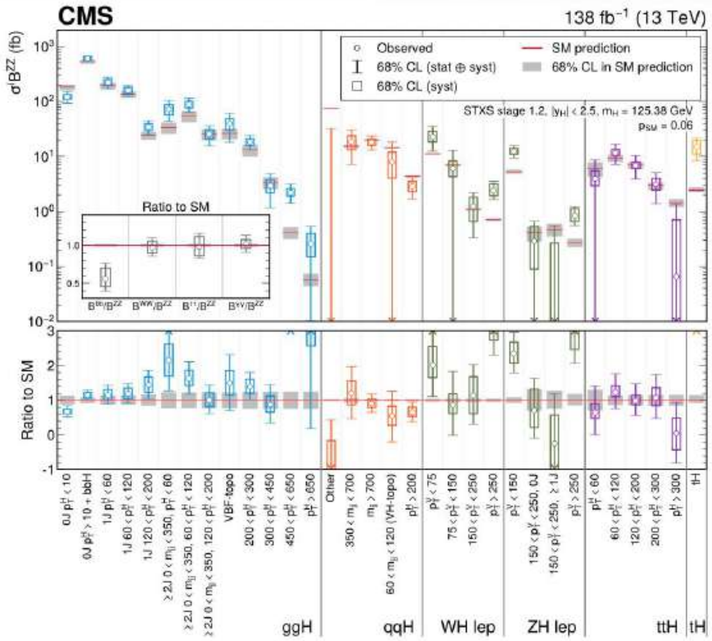

- Precision in several measurements (e.g. ggH 200 < p_T < 300 GeV) now rivals SM theoretical uncertainty
- Experimental data is approaching the point where it can constrain theoretical inputs

CMS-HIG-21-018

κ Coupling Modifiers Interpretation

In kappa framework, $\sigma_i \times B_f$ are expressed in the Narrow-width approximation

$$\sigma_i \times B(H \to f) = \frac{\sigma_i \times \Gamma_f}{\Gamma_H} = \frac{\kappa_i^2 \kappa_f^2}{\kappa_H^2} \sigma_i^{\mathrm{SM}} \times B^{\mathrm{SM}}(H \to f), \qquad \kappa_H^2 = \frac{\sum_f \kappa_f^2 B^{\mathrm{SM}}(H \to f)}{1 - B_i - B_u}$$

κ_F–κ_V model
κ_F, κ_V
- Target: Test global Higgs coupling structure
- Input: On-shell

Resolved κ model
κ_W, κ_Z, κ_t, κ_b, κ_τ, κ_μ, (κ_c)
- Target: Measure direct couplings to SM particles
- Input: On-shell

Effective κ model
Resolved + κ_g, κ_γ, $\kappa_{Z\gamma}$
- Target: Probe BSM effects in loop-induced interactions
- Input: On-shell

BSM-decay constraint
Effective + B_{inv}, B_u
- Target: Constrain BSM effect
- Input: On-shell + Hinv + (Off-shell)

κ-ratio model
$\lambda_{ij} = \kappa_i / \kappa_j$
- Target: Reduce total-width dependence
- Input: On-shell

Width interpretation
Γ_H + couplings
- Target: Constrain the total Higgs width.
- Input: On-shell + Off-shell

κ_λ model
κ_λ + couplings
- Target: Constrain the Higgs self-coupling
- Input: On-shell + Di-Higgs

$m_b(m_H)$ interpretation
$m_b(m_H)$
- Target: Measure the running b-quark mass at the Higgs scale
- Input: On-shell

κ_F- κ_V model with B_{inv} = B_u = 0

CERN-EP-2026-228
(to appear)

- About 10% - 15% improvement in total uncertainties compared to Nature combination
- The observed (expected) correlation between κ_F and κ_V is 40% (36%)
- SM compatibility p_{SM} = 34%

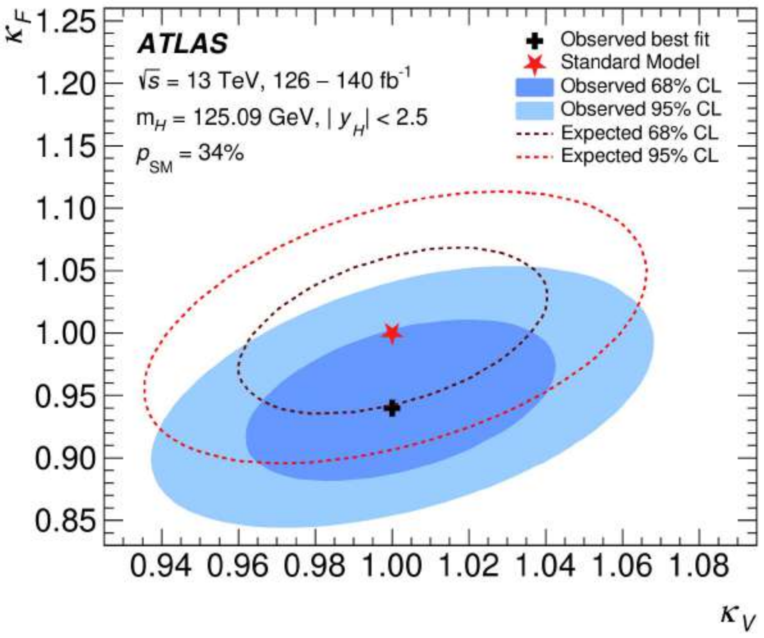

Resolved κ model

$\kappa_W, \kappa_Z, \kappa_t, \kappa_b, \kappa_\tau, \kappa_\mu, (\kappa_c)$

Target	Measure direct couplings to SM particles
Input	On-shell

Resolved κ coupling with $B_{inv} = B_u = 0$

Loop-induced couplings (κ_g, κ_γ, $\kappa_{Z\gamma}$) are resolved assuming no BSM decay (on-shell)

- POIs: κ_W, κ_Z, κ_t, κ_b, κ_τ, κ_μ, (κ_c)

CMS-HIG-21-018

CERN-EP-2026-228

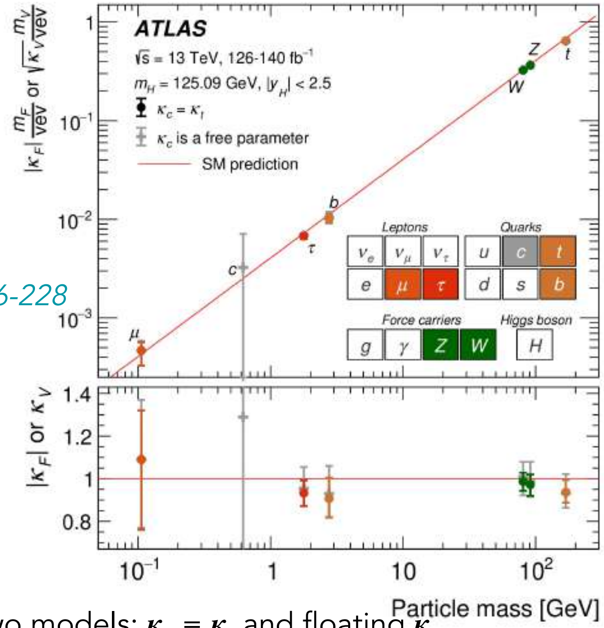

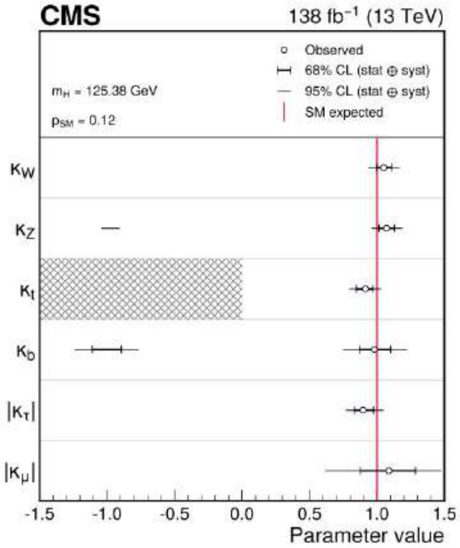

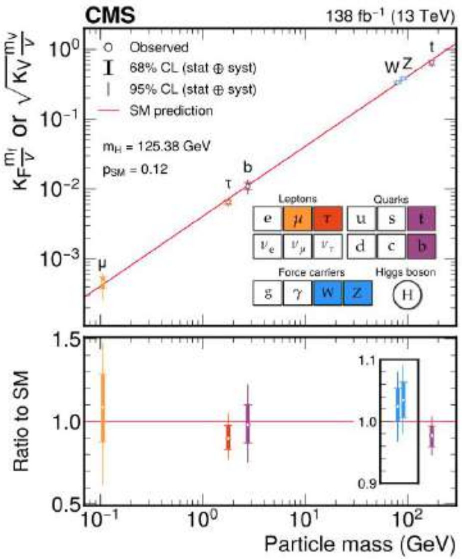

- Two models: $\kappa_c = \kappa_t$ and floating κ_c
- $|\kappa_c| < 4.1$

- κ_t restricted to positive domain
- Best limits on the charm quark coupling: $|\kappa_c| < 3.5$

Effective κ coupling with $B_{inv} = B_{u} = 0$

- Loop-induced couplings treated as independent effective modifiers, assuming no BSM decays (on-shell)
  - POIs: κ_W, κ_Z, κ_t, κ_b, κ_τ, κ_μ, κ_g, κ_λ, (κ_c)
  - Two models fit (κ_c=κ_t and floating κ_c): $\kappa_{Z/W/t/\tau}$ at 5–10% precision, κ_b at 10–15%, κ_c upper limit of 4.2×SM at 95% CL — up to 33% improvement vs. Nature combination,
  - SM compatibility p_{SM} = 70% and 78%

CERN-EP-2026-228
(to appear)

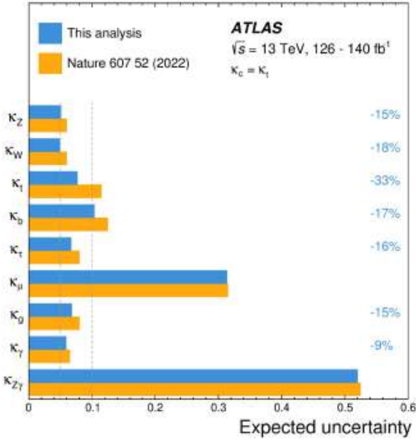

Effective κ model

Resolved + κ_g, κ_γ, $\kappa_{Z\gamma}$

Target	**Probe BSM effects in loop-induced interactions**
Input	**On-shell**

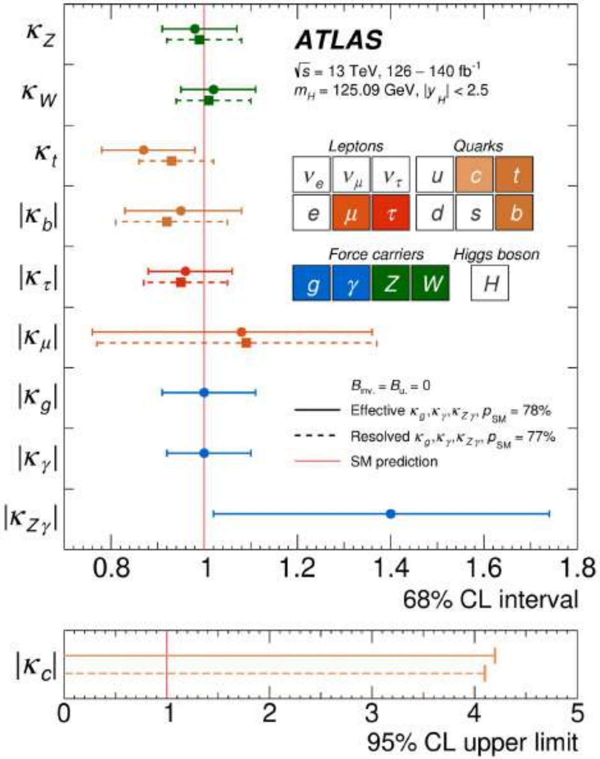

BSM-decay constraint

Effective + B_{inv}, B_u

Target	Constrain BSM effect
Input	On-shell + Hinv + (Off-shell)

BSM-decay constraint

- Loop-induced couplings are treated as independent effective coupling modifiers with floating B_{inv} and B_u
  - POIs: $\kappa_V, \kappa_t, \kappa_b, \kappa_\tau, \kappa_\mu, \kappa_g, \kappa_\gamma, \kappa_{Z\gamma}$, ($\kappa_c$) + ($B_{inv}$, B_u)
- Two extended models:
  - On-shell + Hinv combination assuming $|\kappa_V| \leq 1$
    - Upper limit on B_{inv} of 12.1% at 95% CL
    - Upper limit on B_u of 17.5% at 95% CL
    - SM compatibility p_{SM} = 69%
  - On-shell + Hinv + off-shell combination without additional assumption (remove $H^* \to ZZ^* \to 2\ell 2\nu$ off-shell)
    - Upper limit on B_{inv} of 12% at 95% CL
    - Upper limit on B_u of 32% at 95% CL
    - SM compatibility p_{SM} = 73%

CERN-EP-2026-228
(to appear)

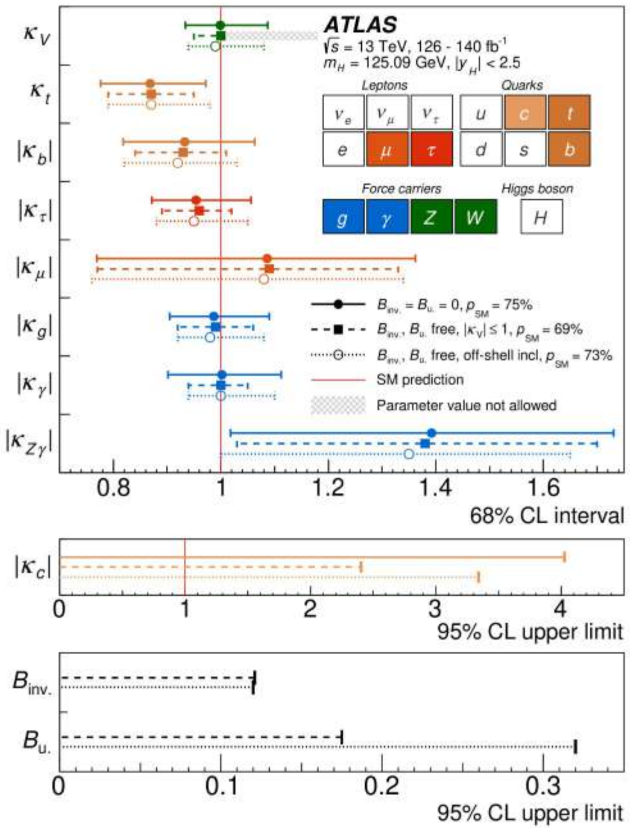

Similar precision in CMS and ATLAS

- EW boson: 5%
- 3rd generation fermion: 10%
- Massless boson: 6-7%
- Invisible BR: < ~ 12%
- Undetected BR: < ~ 30%

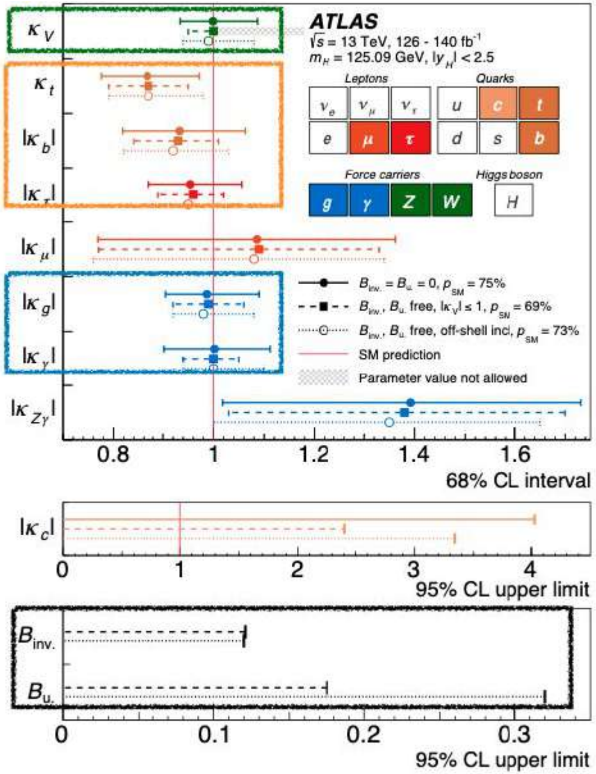

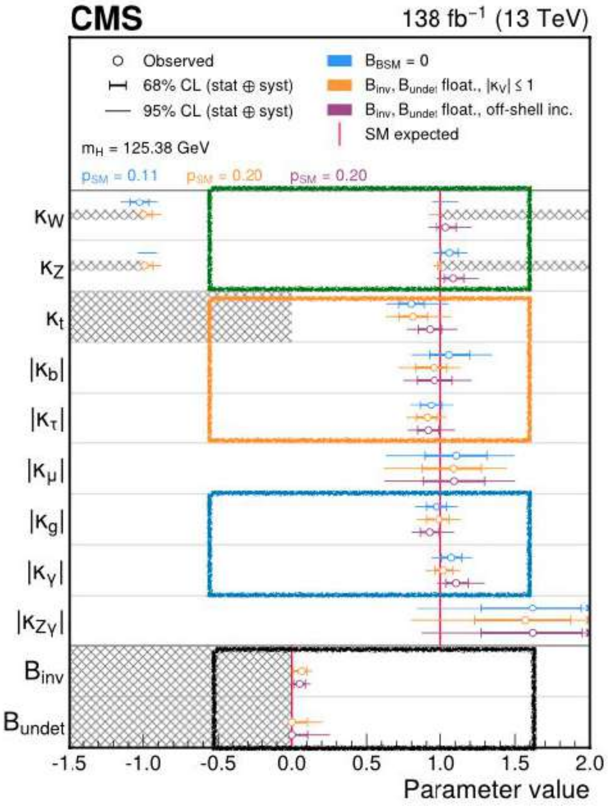

Width interpretation

- Higgs width (Γ_H): sets the Higgs lifetime ($\tau = \hbar/\Gamma_H$); precisely predicted in the SM ($\Gamma_H^{SM} \approx 4.1$ MeV); deviations could signal BSM Higgs decays
- Measured via three approaches:
  - Directly from the Higgs lineshape
  - Indirectly from off-shell production (J. Campbell et al. JHEP 04 (2014) 060)
  - From the Higgs lifetime

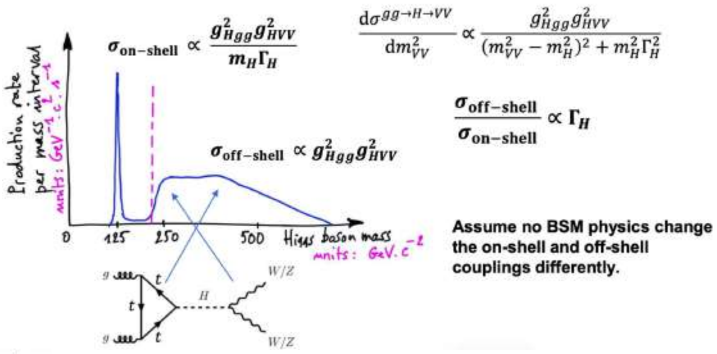

Direct line-shape measurement of H→γγ

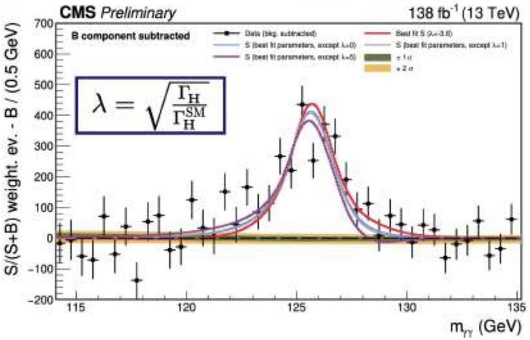

$$\Gamma_H < 92 \text{ MeV at 95\% CL}$$

CMS-HIG-25-004
to appear

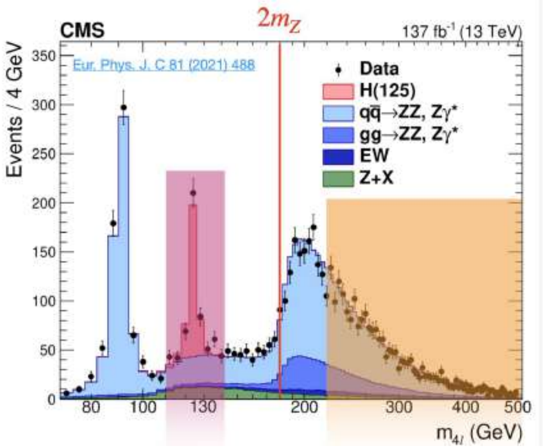

Width results

CERN-EP-2026-228
(to appear)

off-shell and on-shell ZZ+WW

5.0 (2.9)σ on off-shell production

HIG-25-003
to appear

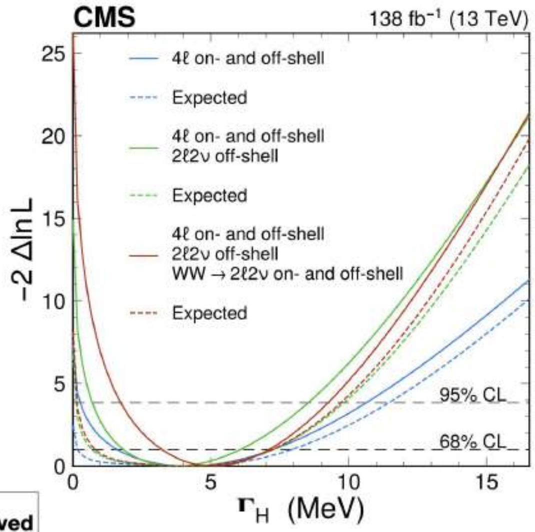

Expected	Observed
$4.1^{+3.1}_{-3.3}$	$5.1^{+2.0}_{-1.8}$

Γ_H Combination (68% CI)

$$\Gamma_H = 5.2^{+2.0}_{-1.8}\ \text{MeV}$$

off-shell includes $H* \rightarrow ZZ$ and $H* \rightarrow WW$ decay channels.

on-shell: All on-shell channels except for $H \rightarrow$ invisible decay.

3.7 (2.9 σ) on off-shell production

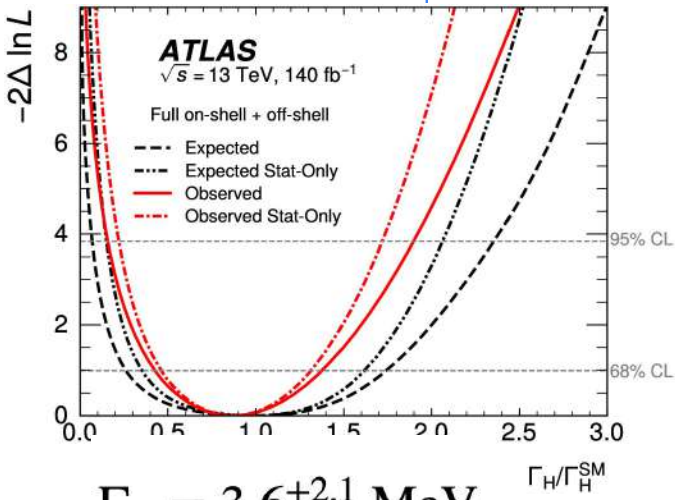

$$\Gamma_H = 3.6^{+2.1}_{-1.6}\ \text{MeV}$$

Expected: $\Gamma_H = 4.1 \pm 3.0$ MeV $= 4.1^{+2.5}_{-2.3}$ (stat.) $^{+1.7}_{-2.0}$ (syst.) MeV @68% *CL*.

Observed: $\Gamma_H = 3.6^{+2.1}_{-1.6}$ MeV $= 3.6^{+1.9}_{-1.4}$ (stat.) $^{+0.9}_{-0.8}$ (syst.) MeV @68% *CL*.

Higgs boson mass (m_H) - CMS

- New three-stage photon energy calibration corrects residual data/MC differences in energy scale and resolution

[CERN-EP-2026-195]

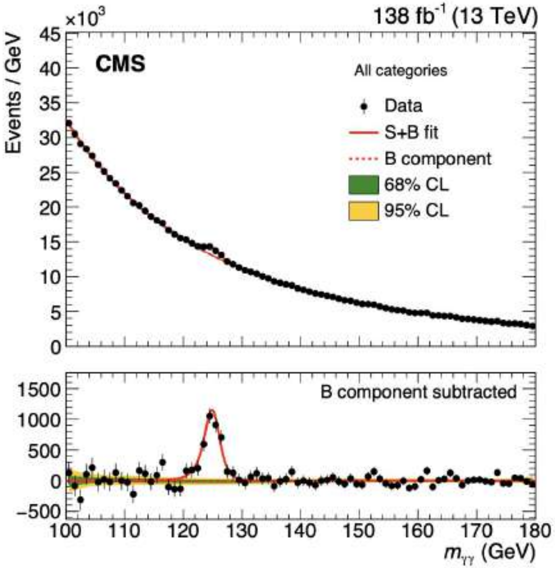

From Z → ee data and MC

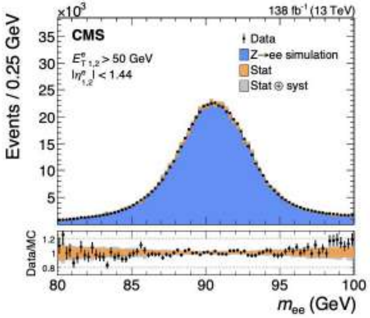

From simulation

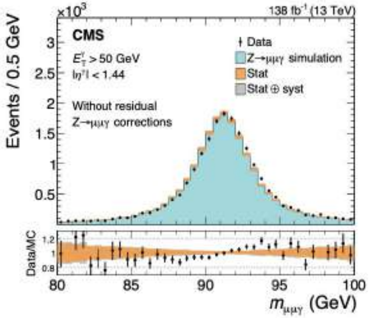

From Z → μμγ data and MC

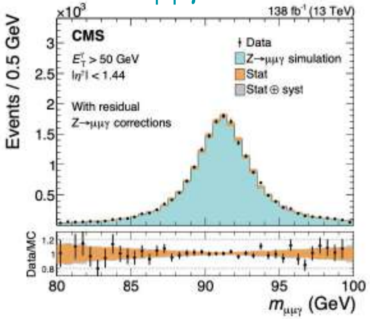

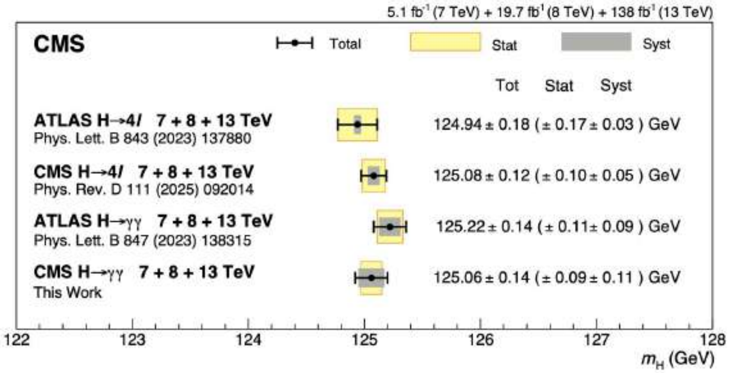

Higgs boson mass (m_H) - ATLAS

$H \rightarrow \gamma\gamma$ 14 categories split by S/B ratio, mγγ, and photon energy scale uncertainty; mH extracted from a simultaneous fit of the mγγ peak across all categories

- Key improvements: optimized categorization, and photon energy scale uncertainty reduced from 320 to 80 MeV

Phys. Rev. Lett. 131 (2023) 251802

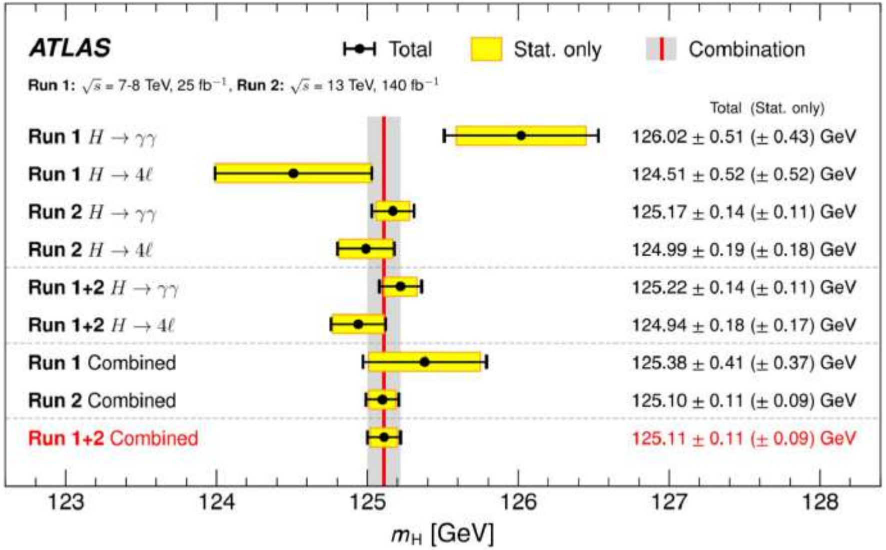

$H \rightarrow ZZ* \rightarrow 4\ell$ 4 final states (4μ, 2e2μ, 2μ2e, 4e), with non-resonant ZZ* as the dominant background

- Signal modelled via PDFs 𝒫(m4ℓ, DNN, σ_i | mH), where DNN discriminates signal from background and σ_i is the per-event m4ℓ resolution estimated by a neural network

Phys. Lett. B 847 (2023) 138315

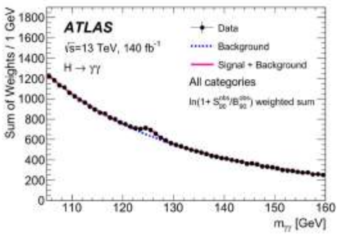

Phys. Lett. B 843 (2023) 137880

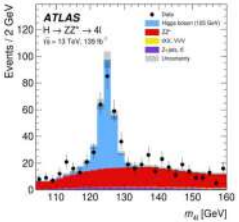

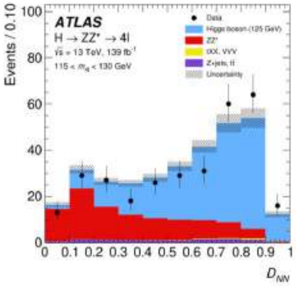

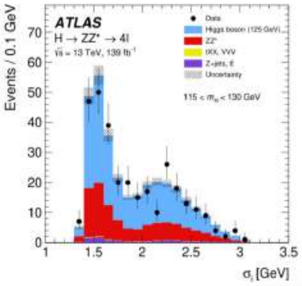

Single Higgs Run 2 (+partial Run 3) results and projections

H→$\mu\mu$ - ATLAS

Rare process: BR = (2.17 ± 0.04) × 10^{-4}

- Large background from Drell-Yan $\mu^+\mu^-$ production
- Extremely small S/B ratio (~O(0.1%)), demanding per-mille-level precision in background modeling

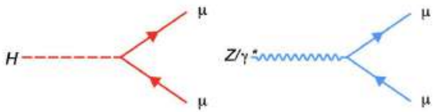

Strategy: Event selection and classification

- Sort events into mutually exclusive categories targeting the various Higgs boson production modes
- Use machine learning to enhance the signal-to-background ratio

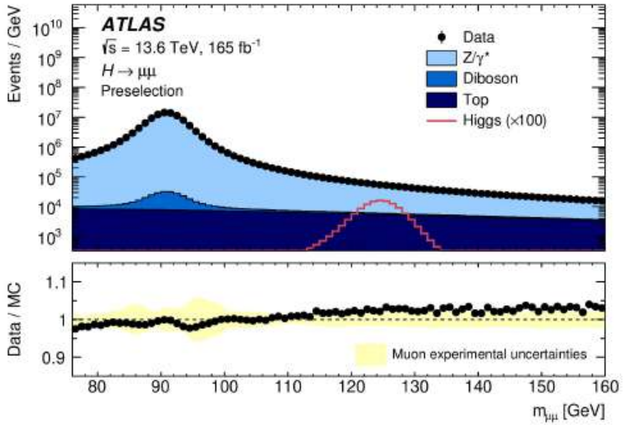

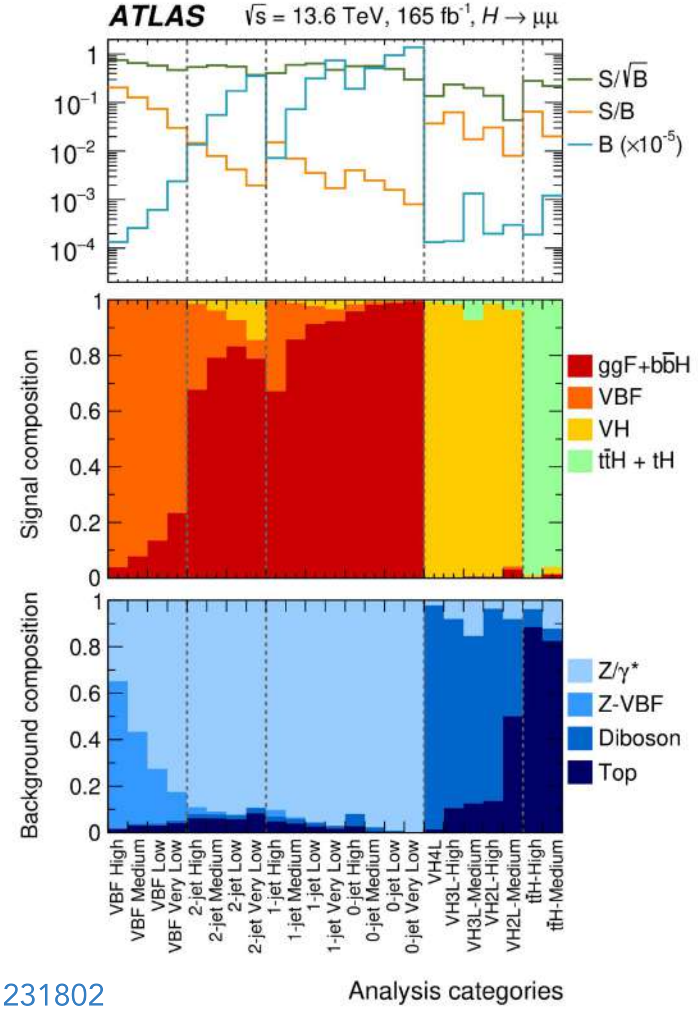

Phys. Rev. Lett. 135 (2025) 231802

Phys. Rev. Lett. 135 (2025) 231802

H→$\mu\mu$ - ATLAS

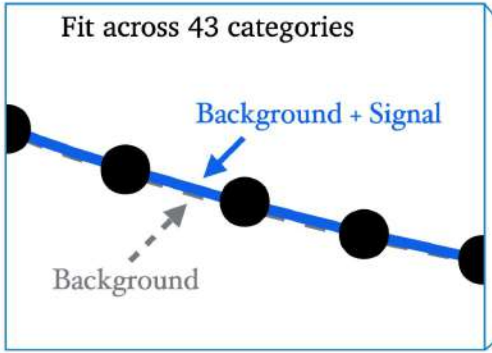

Signal extraction

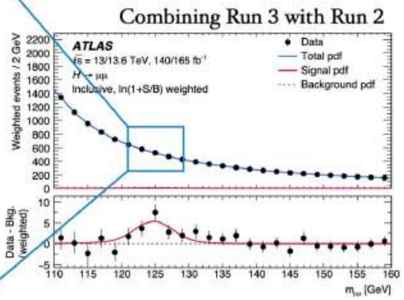

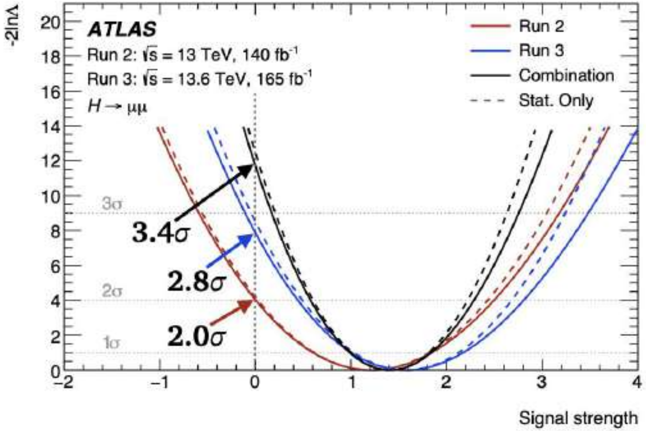

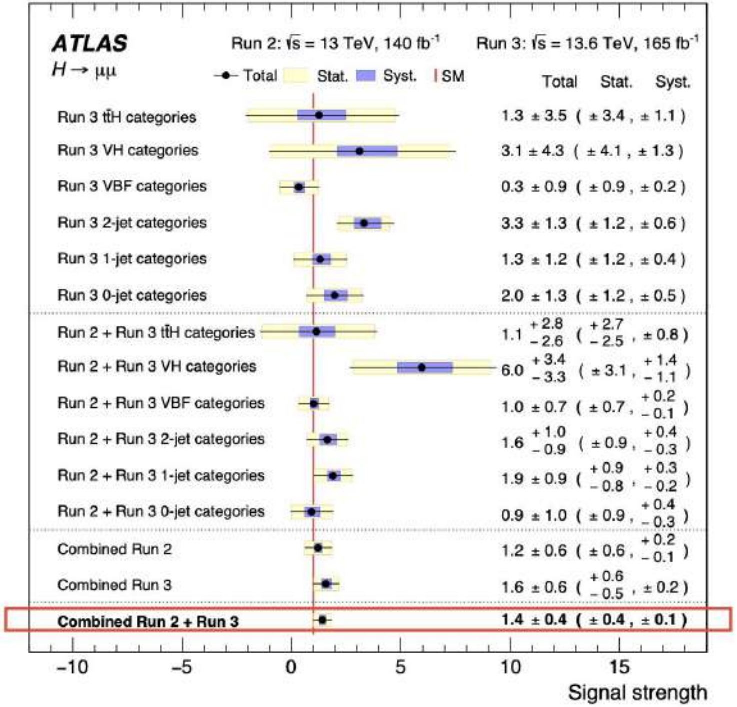

- Significance vs. background-only hypothesis: obs 3.4σ (exp 2.5σ) — combining Run 2 + Run 3 categories (ttH, VH, VBF, 2-jet, 1-jet, 0-jet) improves precision by 50% over Run 2 alone
- Clear evidence for the H→$\mu^+\mu^-$ decay

Phys. Rev. Lett. **136**, 011801

H→cc from ttH production mode - CMS

- First-at-LHC ttH(H→cc̄) search across 0L/1L/2L channels; main challenges are high jet multiplicity and combinatorics
- ParticleNet jet tagger (11 categories, 2× rejection improvement) and Particle Transformer event classifier (10-class, no explicit reconstruction)
- tt̄+HF background constrained via data control regions with floating normalizations, validated using ttZ(Z→cc/bb)

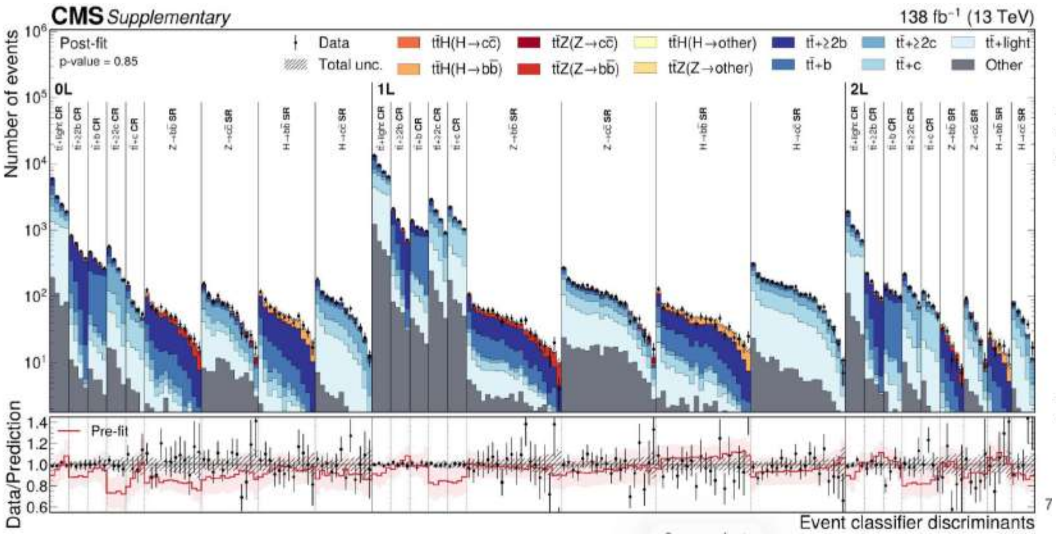

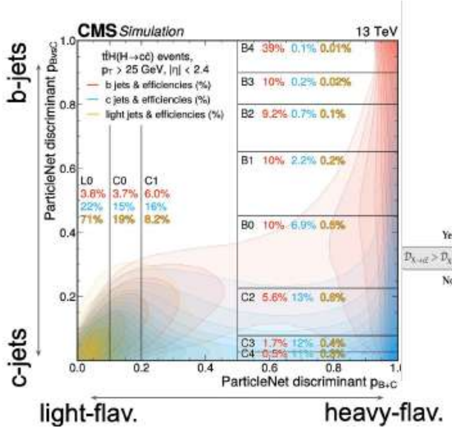

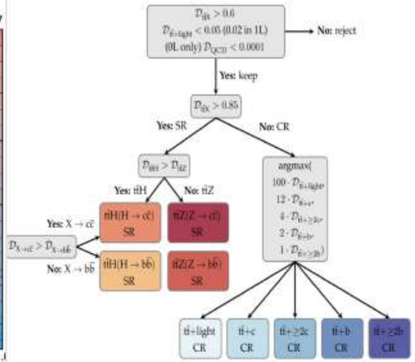

Phys. Rev. Lett. **136**, 011801

H→cc from ttH production mode - CMS

Signal strength	Best fit	Obs (Exp) significance
ttH→bb	0.9 +0.3/-0.2	4.4σ (4.5σ)
ttH→cc	-1.6 ± 4.5	–
ttZ→bb	1.5 ± 0.4	3.5σ (2.4σ)
ttZ→cc	1.0 ± 0.8	1.2σ (1.3σ)

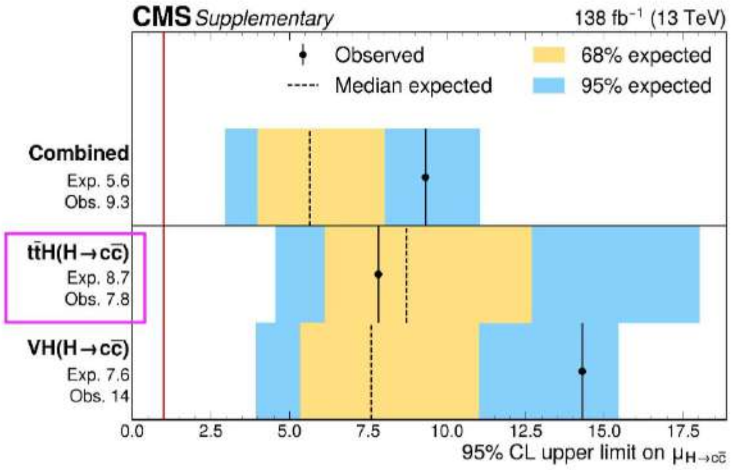

Exp. sensitivity comparable to VH→cc search

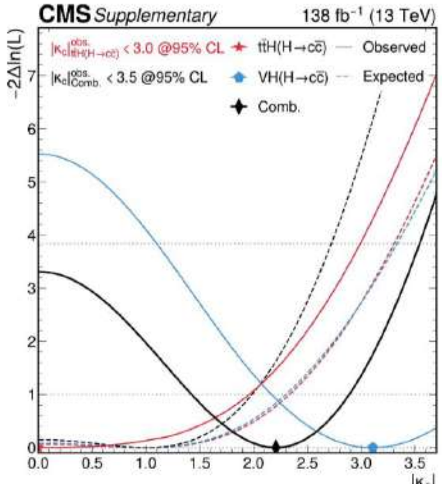

Combining ttH+VH: $\kappa_c < 3.5$

H→cc from VBF production mode - ATLAS

H→cc:

- μ_cc = 18 ± 13 → μ_cc < 41 (28 expected) at 95% CL; VBF+VH gives 𝜿_c < 4.7 (3.9 expected) — an 8% improvement over VH alone

H→bb:

- μ = 0.97 (+0.57/−0.50);
- combination with Run 2 reaches 3.2σ, giving first evidence for VBF H→bb

CERN-EP-2025-247

Both channels remain statistically limited

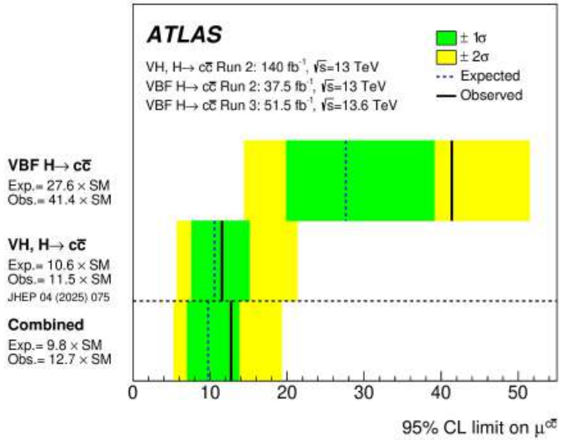

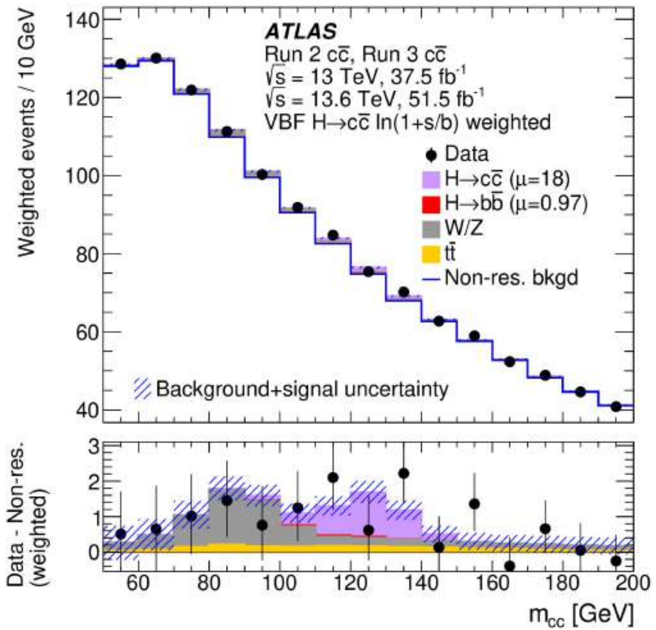

H→cc coupling @ HL-LHC

Run 2 constraints:
CMS: ttH + VH, $\kappa_c < 3.5$
ATLAS: VH + VBF, $\kappa_c < 4.7$

Projections based on Run 2 analyses predict ~2σ significance at 3000 fb^{-1}

- Further gains expected from detector upgrades: high-precision timing info for jet tagging, and tracking info available at the first trigger stage
- ML-driven improvements continue to enhance both jet tagging and analysis techniques

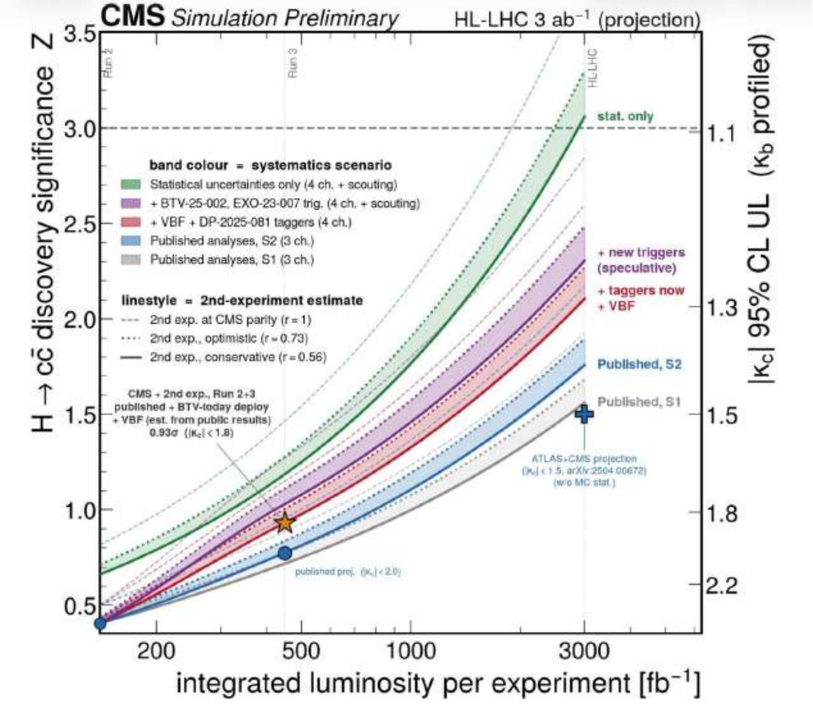

Public analyses lumi scale ~ 1.8σ
Known improvement (tagger and trigger) ~ 2.3σ

Couplings projections @ HL-LHC

ATL-PHYS-PUB-2025-018
CMS-HIG-25-002

Expect to reach < 2% precision
for most of the couplings at 3 ab^{-1}

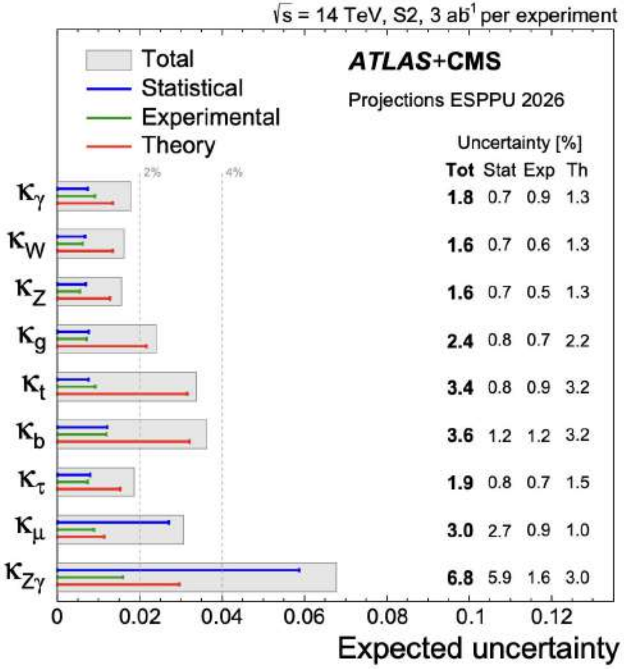

$\sqrt{s}$ = 13 TeV	YR4	YR5
σ	48.58 pb	48.09 pb
δ(scale)	$^{+0.21\%}_{-2.37\%}$	$^{+0.29\%}_{-3.33\%}$
δ(EWK)	$\pm1\%$	$\pm1\%$
$\delta(t,b,c)$	$\pm0.83\%$	$\pm0.34\%$
$\delta(1/m_t)$	$\pm1\%$	0
δ(trunc)	$\pm0.37\%$	0
δ(theory)	$^{+3.41\%}_{-5.57\%}$	$^{+1.63\%}_{-4.67\%}$
$\delta(\mathrm{PDF}+\alpha_s)$	$\pm3.2\%$	$^{+2.69\%}_{-2.28\%}$
δ(PDF-TH)	$\pm1.16\%$	$\pm2.31\%$

LHC Higgs Working Group ReportsReport 5

Ongoing efforts from the theory community are expected to further improve the precision.

Constraints on effective field theory models

- EFT offers a model-independent way to probe new physics beyond direct LHC reach, via higher-dimensional SMEFT operators
- These SMEFT effects alter Higgs production and decay rates

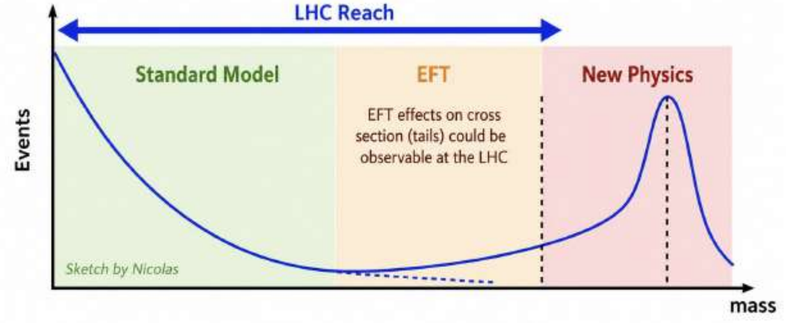

$$\mathcal{L} = \mathcal{L}_{\text{SM}} + \sum_i c_i^{(6)} O_i^{(6)} / \Lambda^2$$

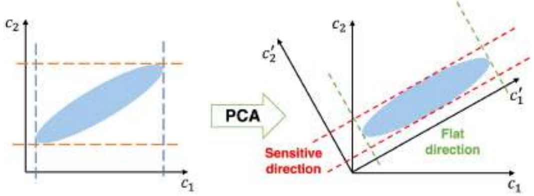

Constraints on effective field theory models - CMS

- New physics may shift multiple Wilson coefficients at once, causing large degeneracies and flat, hard-to-fit likelihood surfaces
- PCA identifies the sensitive directions, enabling a simultaneous fit to 17 linear combinations of WCs

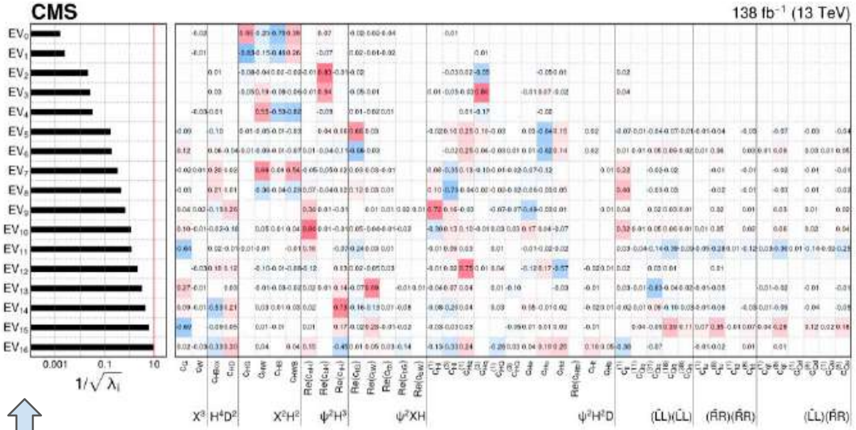

[CMS-HIG-21-018](#)

- $1/\lambda_j$ for each eigenvector, where λ_j is the corresponding eigenvalue.

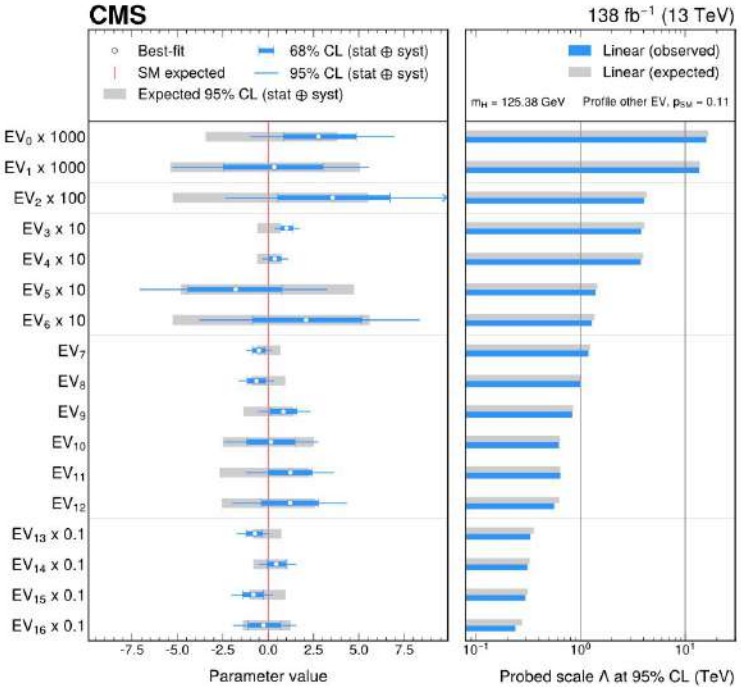

- Constraints on the linear combinations of SMEFT WCs extracted with the PCA procedure.

Constraints on effective field theory models - ATLAS

- Fit performed at Λ = 1 TeV; both linear and linear+quadratic results produced
- Up to 55% tighter constraints than the Nature combination; results consistent with the SM, no significant deviations

CERN-EP-2026-228

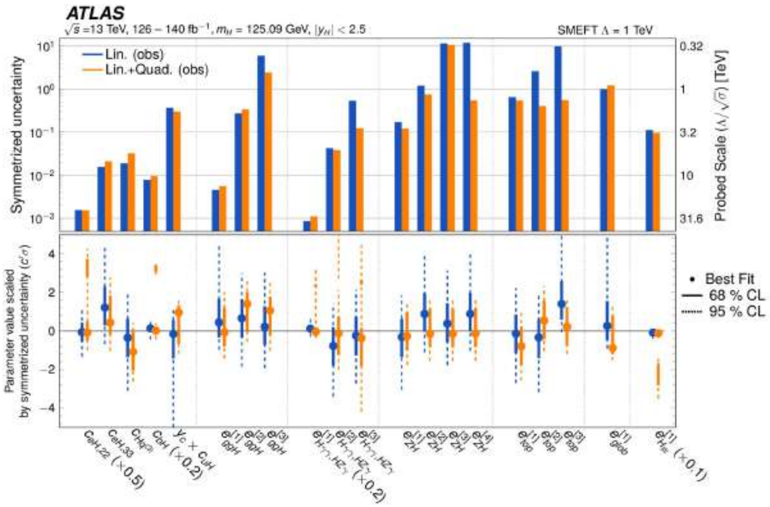

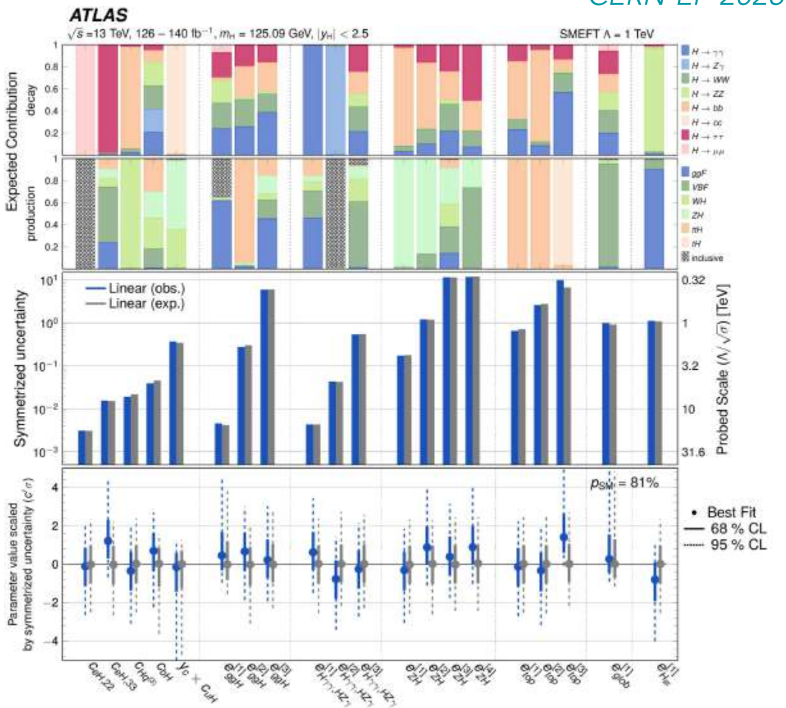

Extracting κ_λ through NLO electroweak corrections

- Single-Higgs (indirect, via NLO EW corrections) combined with di-Higgs (direct) tightens the κ_λ constraint vs. di-Higgs alone
- Two scenarios:
  - Only floating κ_λ (others fixed)
    - about 25% (20%) compared with di-Higgs only
  - Generic: floating κ_λ and κ_V, κ_t, κ_b, κ_τ
    - about 1% and 5% after floating all κ , showing the combination is robust to fewer assumptions

$\kappa_\lambda = \lambda_{HHH}/\lambda_{HHH}^{SM}$

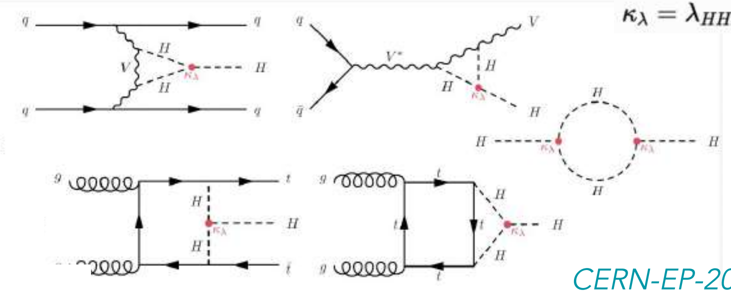

CERN-EP-2026-228

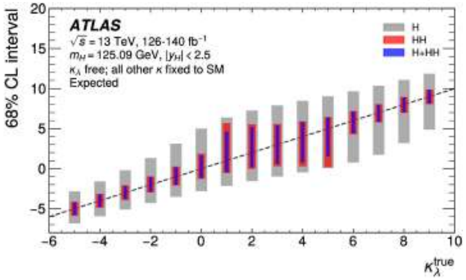

Fit	Best fit	68% CL interval	95% CL interval
Single-Higgs	$-0.9^{+3.9}_{-2.5}$	[−3.4, 3.0]	[−5.3, 8.8]
Di-Higgs	$3.5^{+2.4}_{-3.4}$	[0.1, 5.9]	[−1.3, 7.2]
H+HH (others fixed)	$1.3^{+3.1}_{-1.6}$	[−0.3, 4.4]	[−1.5, 6.5]
H+HH (generic)	$0.6^{+2.5}_{-1.5}$	[−0.9, 3.1]	[−2.1, 5.9]

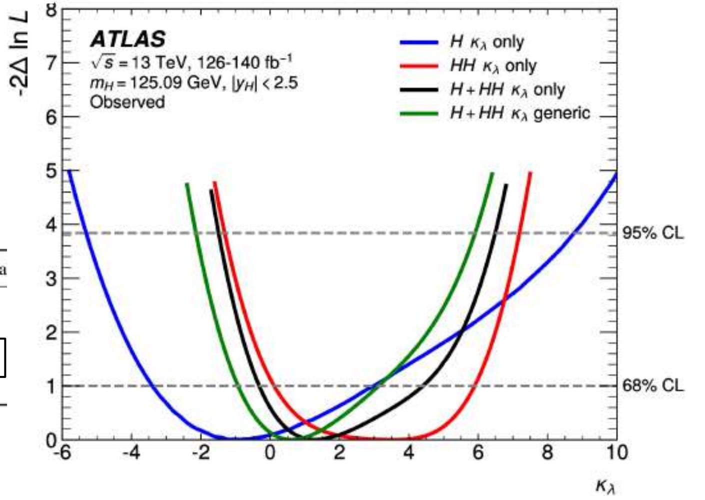

Di-Higgs searches

The Higgs potential and Di-Higgs searches

- Potential shape and origin are experimentally very loosely unconstrained
- Local minimum established since 2012
- Key predictions to consolidate our understanding of the EW symmetry breaking mechanism and the evolution of the Universe

$$V(H) = \frac{1}{2} m_H^2 H^2 + \lambda_3 \nu H^3 + \frac{1}{4} \lambda_4 H^4$$

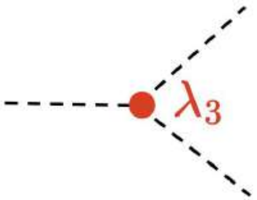

accessible via HH production

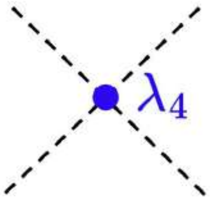

accessible via HHH production

$$\lambda_3 = \lambda_4 = \lambda \text{ in the SM}, \quad \kappa_\lambda = \frac{\lambda}{\lambda_{SM}}$$

Nature Reviews Physics **3**, 608–624 (2021)

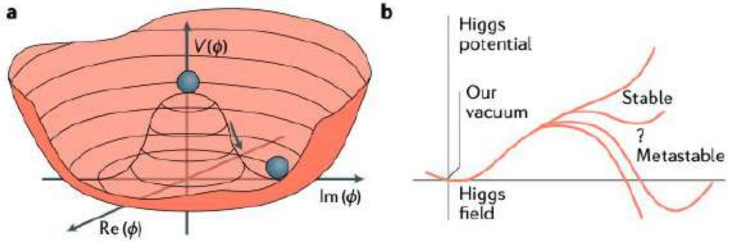

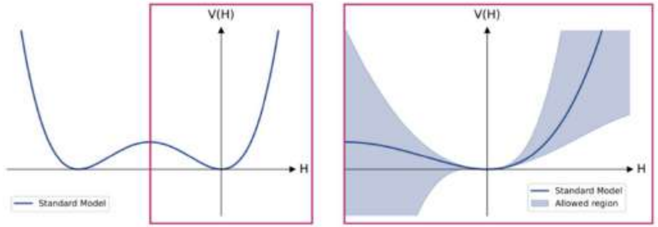

what the SM predicts

what we know experimentally using ATLAS Run 2 legacy limits @95%CL

- Measure **HH** to probe the potential shape by determining the **strength** of Higgs boson self-couplings

HH production at LHC

- Destructive interference between the box and the triangle diagrams
- Cross section is suppressed (~10^3 times smaller than that of single Higgs cross section)
- Deviations from SM can increase this cross section

$\sigma_{ggF} \approx$ 31 (34) fb @ 13 (13.6) TeV

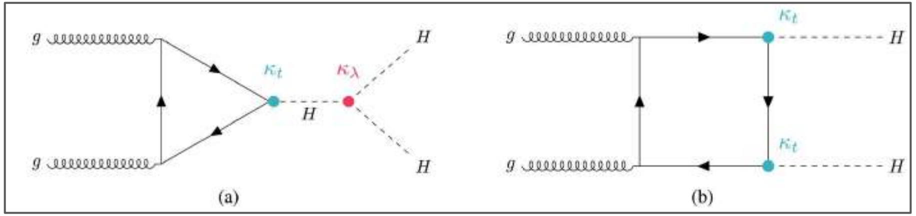

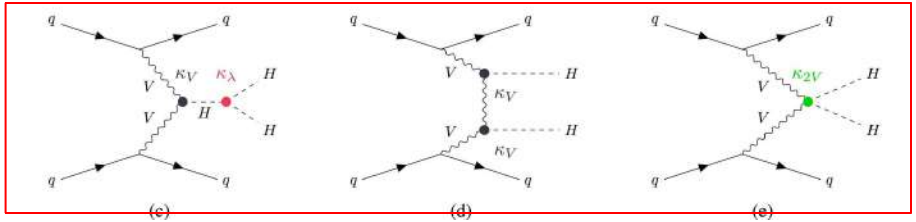

$\sigma_{VBF} \approx$ 1.7 (1.9) fb @ 13 (13.6) TeV

Reviews in Physics (2020)

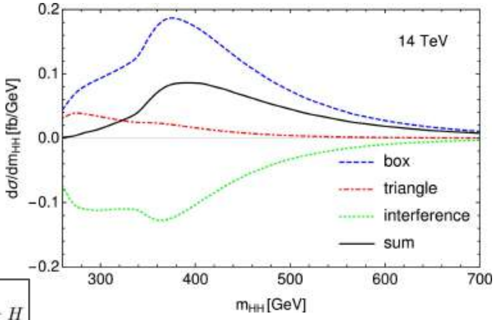

Phys.Lett. B732 (2014) 142-149

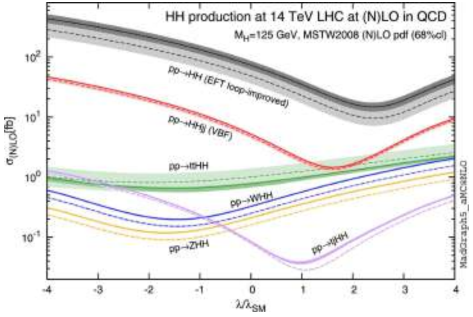

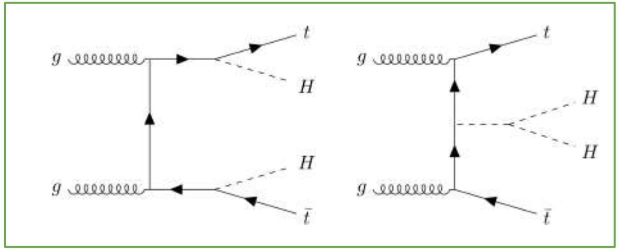

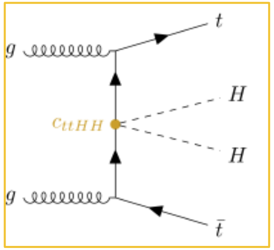

$\sigma_{ttHH} \approx$ 0.7 (0.9) fb @ 13 (13.6) TeV

EFT quartic coupling

HH ATLAS+CMS Run 2 combination

- Both ATLAS and CMS have a broad physics program to cover many decay mod
  - Compromise between purity and BR
  - VV channels mainly exploited through electron / muon decay channels
  - require excellent performance from all physics objects

	bb	WW	ττ	ZZ	γγ
bb	34%				
WW	25%	4.6%			
ττ	7.3%	2.7%	0.39%		
ZZ	3.1%	1.1%	0.33%	0.069%	
γγ	0.26%	0.10%	0.028%	0.012%	0.0005%

[CERN-EP-2026-011 Submitted to Phys. Rev. Lett.]

	Channel	Details	Expected			Observed		
			μ_{HH}	κ_λ	κ_{2V}	μ_{HH}	κ_λ	κ_{2V}
ATLAS	bbbb	[36, 38]	< 8.1	[−5.3, 12]	[0.38, 1.7]	< 5.4	[−3.4, 11]	[0.55, 1.5]
ATLAS	$bb\tau\tau$	[40]	< 3.3	[−2.6, 9.2]	[−0.24, 2.4]	< 5.8	[−3.3, 9.1]	[−0.51, 2.7]
ATLAS	$bb\gamma\gamma$	[42]	< 5.2	[−3.0, 7.9]	[−1.1, 3.3]	< 4.1	[−1.6, 7.0]	[−0.48, 2.7]
ATLAS	$bb\ell\ell + E_T^{miss}$	[44]	< 14	[−11, 17]	[−0.50, 2.7]	< 9.6	[−6.5, 13]	[−0.19, 2.4]
ATLAS	Multilepton	[51]	< 11	[−4.5, 9.6]	[−1.9, 4.1]	< 17	[−6.4, 12]	[−2.5, 4.7]
ATLAS	Combined	[48]	< 2.4	[−1.7, 7.2]	[0.41, 1.7]	< 2.9	[−1.3, 7.2]	[0.57, 1.5]
CMS	bbbb	[35, 37]	< 4.3	[−4.6, 12]	[0.63, 1.4]	< 7.0	[−5.0, 12]	[0.66, 1.4]
CMS	$bb\tau\tau$	[39]	< 5.4	[−4.2, 11]	[−0.64, 2.8]	< 3.5	[−1.9, 8.9]	[−0.32, 2.5]
CMS	$bb\gamma\gamma$	[41]	< 5.7	[−3.5, 8.8]	[−0.94, 3.1]	< 8.7	[−3.5, 8.0]	[−1.4, 3.6]
CMS	bbWW	[43]	< 19	[−9.4, 16]	[−1.4, 3.5]	< 15	[−6.1, 13]	[−1.0, 3.1]
CMS	Multilepton	[50]	< 20	[−8.0, 12]	[−2.5, 4.6]	< 22	[−5.8, 10]	[−3.4, 5.6]
CMS	Combined	[49]	< 2.6	[−2.2, 8.0]	[0.63, 1.4]	< 3.5	[−1.4, 6.6]	[0.66, 1.4]
ATLAS + CMS combined			< 1.7	[−1.3, 6.7]	[0.66, 1.4]	< 2.5	[−0.71, 6.1]	[0.73, 1.3]

- A large variety of analysis strategies:
  - very complex analyses with multiple SR targeting multiple production modes simultaneously
- Recent ATLAS+CMS combination
  - Covers most decay channels
- Complementary constraints on $\boldsymbol{\kappa_\lambda}$, $\boldsymbol{\kappa_{2V}}$, and $\boldsymbol{\mu_{HH}}$

HH ATLAS+CMS Run 2 combination

- Observed (expected) HH signal significance: 1.1 (1.3) σ

$$\hat{\mu}_{HH} = 0.8^{+0.9}_{-0.7} = 0.8^{+0.7}_{-0.6}(\text{stat.})^{+0.4}_{-0.2}(\text{theory})^{+0.3}_{-0.3}(\text{exp.})$$

- Important improvements are on the way to reach an evidence with run 3 data
    - Largely dominated by statistics

- Statistical combination of Run 2 results:
    - equalising signal predictions among experiments
    - understanding correlated uncertainty source
    - reproducing results with each-others frameworks

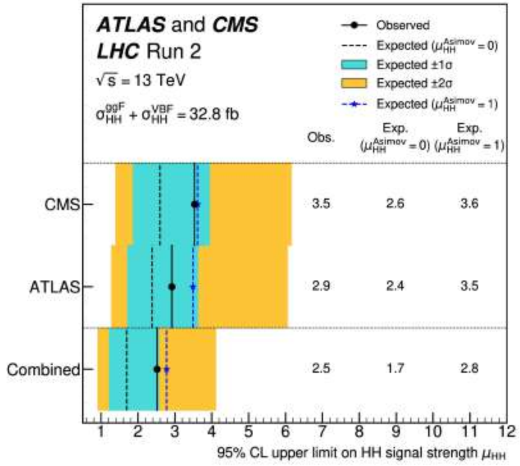

$-0.71 < \kappa_\lambda < 6.1$ @ 95%CL

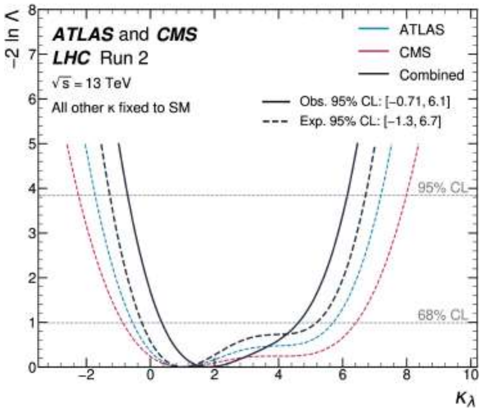

$0.73 < \kappa_{2V} < 1.3$ @ 95%CL

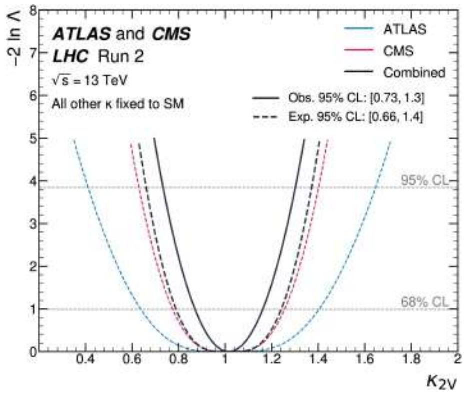

Run 3 opportunities and challenges

Opportunities: new data, upgraded detectors, more powerful AI-powered algorithms, new triggers
Challenges: harsher conditions, understanding detector performance, aging detectors, bookkeeping

Nature Communications 541 (2026)

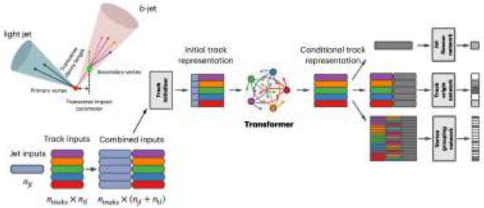

CERN-EP-2026-101

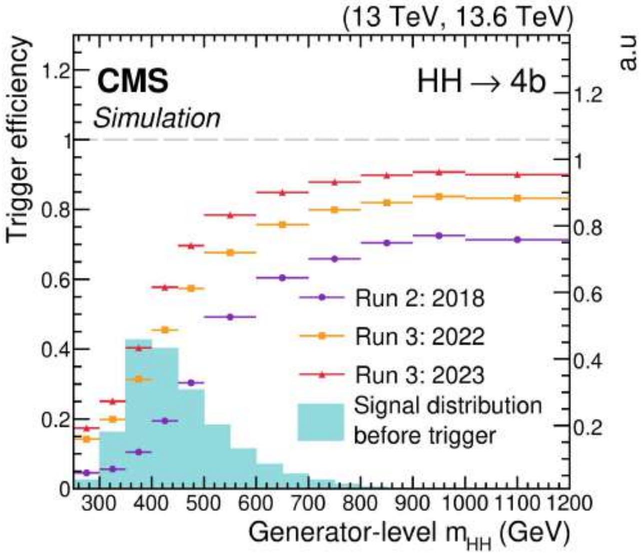

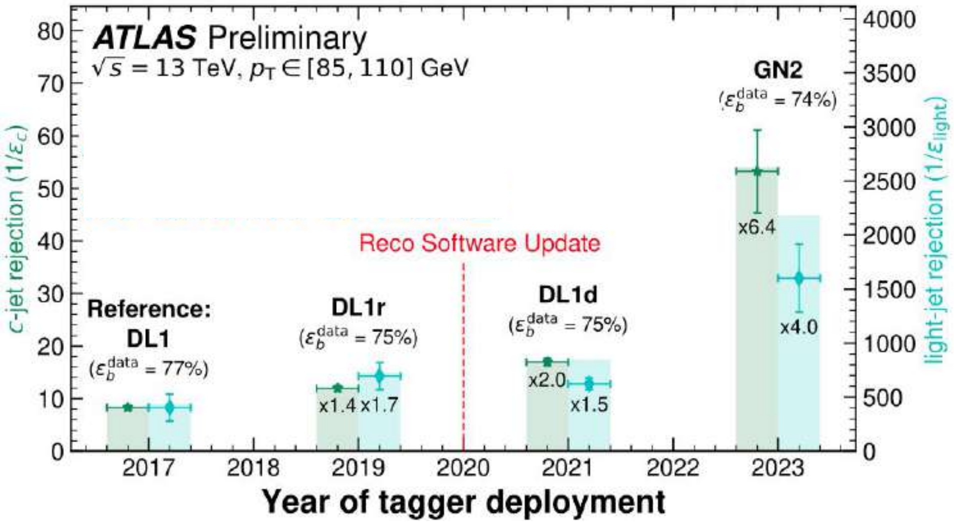

Signal efficiency: **18%** → **45%**

Run 3 AI - powered: featuring HH→bb$\tau\tau$

ATLAS

CERN-EP-2026-227

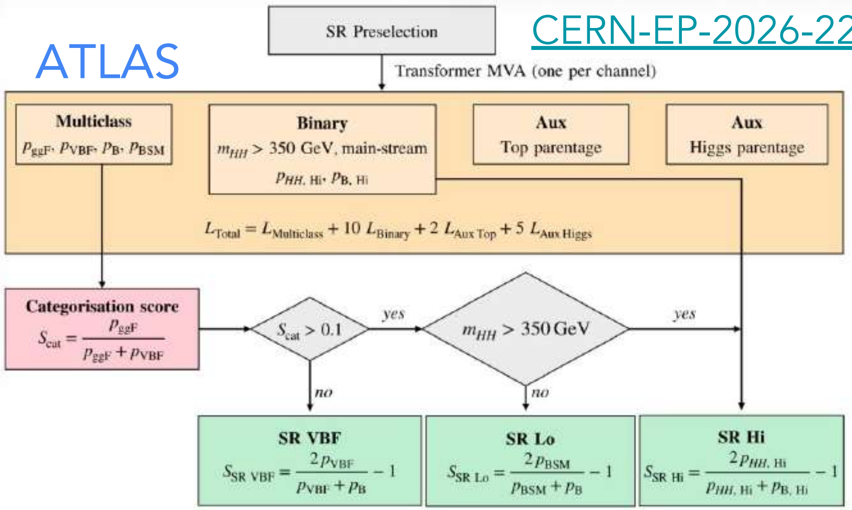

- b-jets: state-of-the-art GN2 b-tagging (85% efficiency); τhad: RNN-based τ-tagging with better electron-fake rejection and a re-optimized MMC algorithm for mττ; trigger: new lower-pT thresholds in Run 3 improve signal acceptance
- New transformer-based model combines event- and object-level variables to output classification scores plus auxiliary top/Higgs origin predictions per object

- New/expanded triggers: 2τ+1 jet, 4-jet parking (1τ+1 b-tag), and extensive VBF parking triggers, plus a dedicated DNN for VBF jet selection
- Improved signal extraction via a new DNN architecture combining a Lorentz-Boosted Network (feature extraction), a ττ-mass regression network, and a DenseNet classifier

CMS

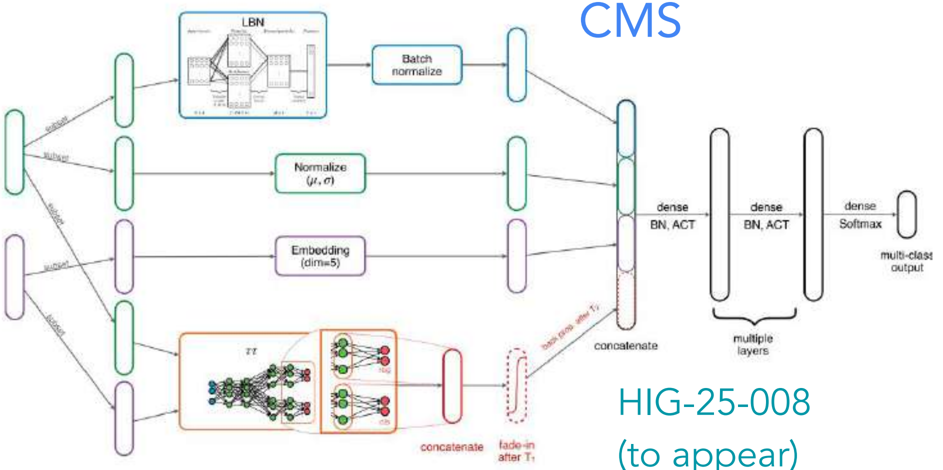

HIG-25-008 (to appear)

Recent Run 2 + partial Run 3 results

HH → bbbb - CMS ($\mathscr{L}$ = 138 + 62 fb^{-1})

- NN multi-classifiers (various architectures) separate ggF/VBF HH signal from data-driven background, using jet and di-jet 4-vector inputs
- SvsB discriminant bins are uniform in signal

Obs $-4.1 < \kappa_\lambda < 9.6$

Obs $0.77 < \kappa_{2V} < 1.27$

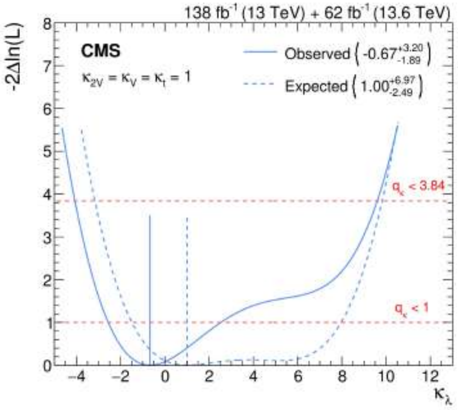

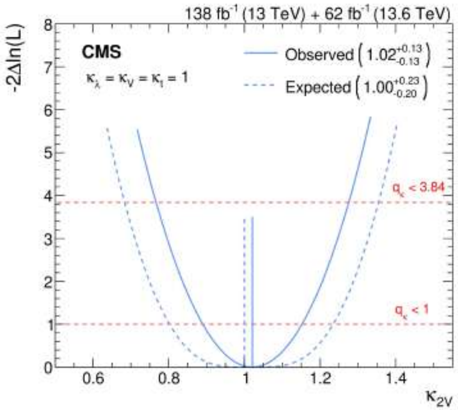

Most stringent constraints on κ_{2V} to date

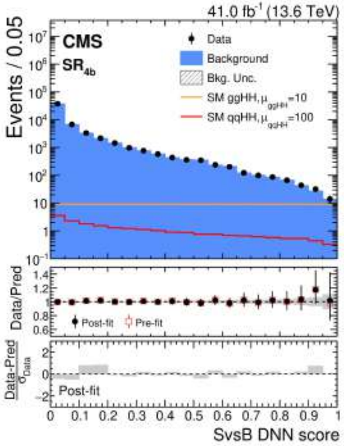

Best sensitivity achieved in the HH → 4b final state to date

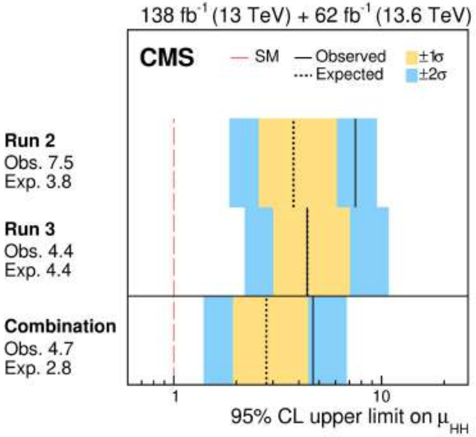

Statistical combination of Run 2 and Run 3 performed with:

- Resolved and boosted topologies with Run 3 data
- Re-analysis of Run 2 resolved topology
- Run 2 boosted analysis

HH → bbγγ - ATLAS ($\mathscr{L}$ = 140 + 168 fb^{-1})

- Di-photon trigger [Phys. Lett. B 876 (2026) 140280]
- $105 < m_{\gamma\gamma} < 160$ GeV
- ≥2 b-jets @85% ID efficiency
- Kinematic fit to improve m_{bb} (constrained by $m_{\gamma\gamma}$)
- Two BDT in low and high $m^*_{bb\gamma\gamma}$ regions
  - Trained with a mixture of SM and BSM samples
- Fit $m_{\gamma\gamma}$ in 14 BDT categories

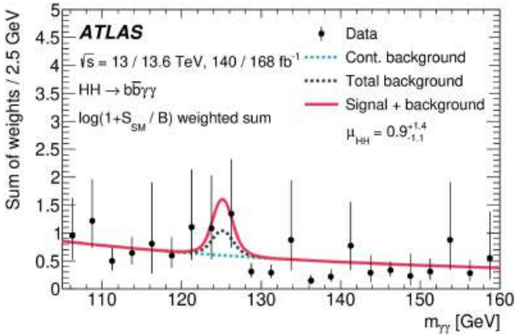

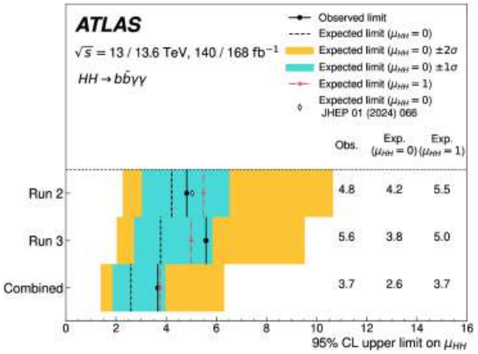

$$\mu_{HH} = 0.9^{+1.4}_{-1.1} = 0.9^{+1.3}_{-1.0}\,(\text{stat.}) \pm 0.5\,(\text{syst.})$$

- Observed (expected) significance 0.87 (1.1) σ — a factor ~2 improvement over Run 2 (from more data, b-tagging, BDT categories, kinematic fit),
- limited by statistics, signal modeling, and photon energy scale

Obs $-1.6 < \kappa_\lambda < 6.6$

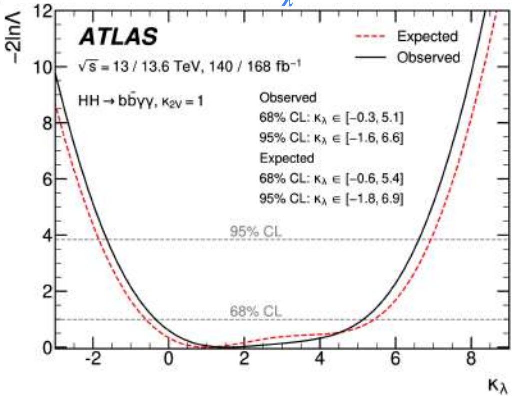

Obs $-0.5 < \kappa_{2V} < 2.6$

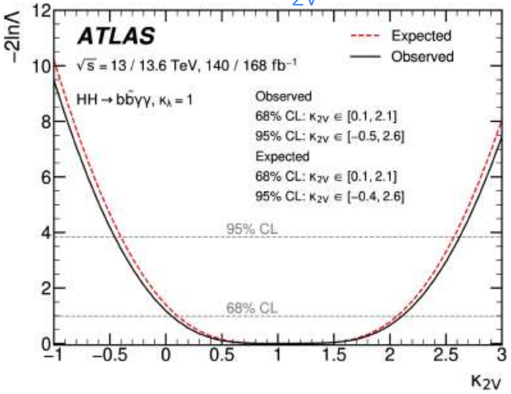

HH→bbττ - ATLAS (ℒ = 140+56 fb^{-1})

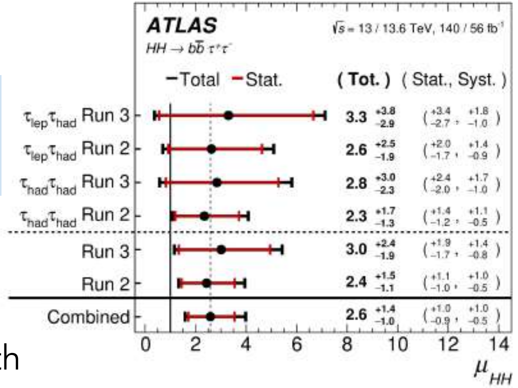

- $\tau_{had}\tau_{had}$ + $\tau_{lep}\tau_{had}$: same overall strategy as Run 2 legacy, but with the BDT replaced by a transformer;
- Event selection: $\tau_{had}\tau_{had}$ triggers on $\tau_{had(s)}$ or b-jets, requires 2 b-jets + 2τ_{had} (no e/μ); $\tau_{lep}\tau_{had}$ triggers on the lepton, requires 2 b-jets + 1 e/μ + 1τ_{had} — both with m_{bb} and $m_{\tau\tau}$ requirements
- Measurement statistically dominated
- Leading systematics: ggF HH and H modelling/ttbar-tW interference modelling
- observed (expected) significance 2.6 (1.2) σ — a ~60% sensitivity gain over Run 2 legacy, with ~1.65σ above the SM expectation

$$\mu_{HH} = 2.6^{+1.4}_{-1.0} = 2.6^{+1.0}_{-0.9}\,(\text{stat.})^{+1.0}_{-0.5}\,(\text{syst.})$$

CERN-EP-2026-227

Run 2

Run 3

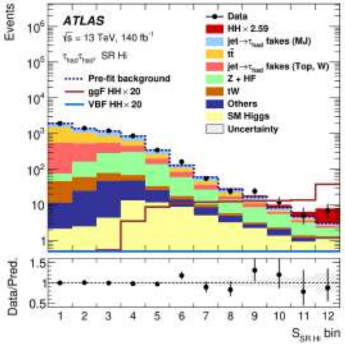

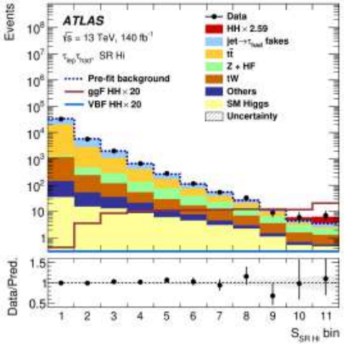

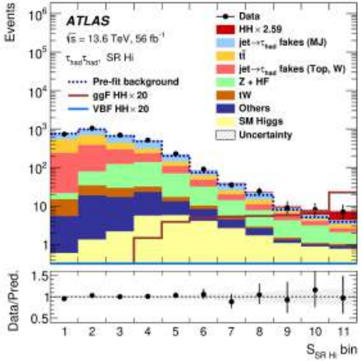

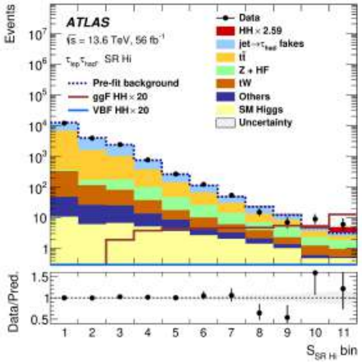

$\tau_{had}\tau_{had}$ more sensitive than $\tau_{lep}\tau_{had}$

Run 2 SRs (high-m_{HH}) outperform Run 3 SRs, (larger ℒ)

HH→bbττ - ATLAS (ℒ =140+56 fb^{-1})

Obs κ_λ [−3.4,1.6] ∪ [5.5,10.1]

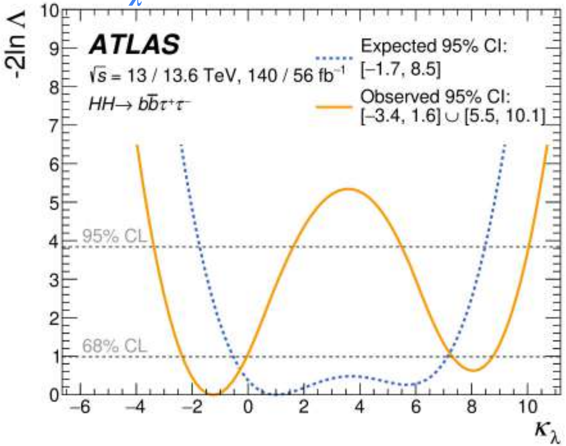

Obs κ_{2V} [−0.2,2.4]

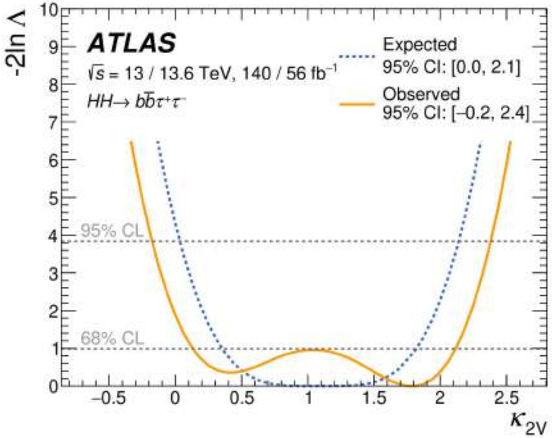

CERN-EP-2026-227

Expected μ_{HH} upper limit (2.4) is now equivalent to the full ATLAS Run 2 combination

Double minimum shape caused by the quadratic dependence of the cross-section on κ_λ and κ_{2V}

Phys.Rev.Lett. 133,101801

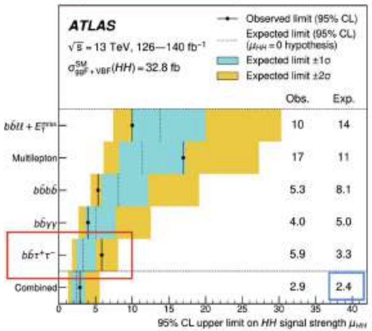

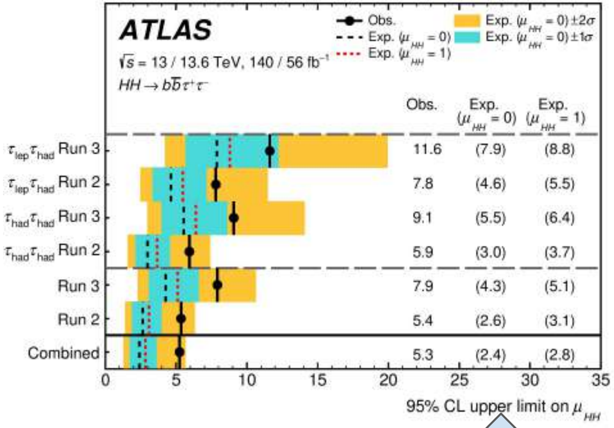

Auxiliary ZH/ZZ→bbττ measurements - ATLAS ($\mathscr{L}$ =140+56 fb^{-1})

- ZH/ZZ → bbττ used as standard candles to validate HH analysis CERN-EP-2026-227
- Result obtained by changing the output score to target ZH/ZZ instead of HH, using the same analysis chain, in the m_{HH} > 350 GeV regions
- Obs (exp) significance: 1.8 (2.7) σ
- Obs (exp) significance: 3.5 (2.4) σ
- Results are compatible with SM (μ=1) at ~1σ

$$\mu_{ZH} = 1.52^{+0.52}_{-0.48} = 1.52 \pm 0.40\,(\text{stat.})^{+0.33}_{-0.28}\,(\text{syst.})$$

$$\mu_{ZZ} = 0.64^{+0.39}_{-0.36} = 0.64 \pm 0.28\,(\text{stat.})^{+0.25}_{-0.28}\,(\text{syst.})$$

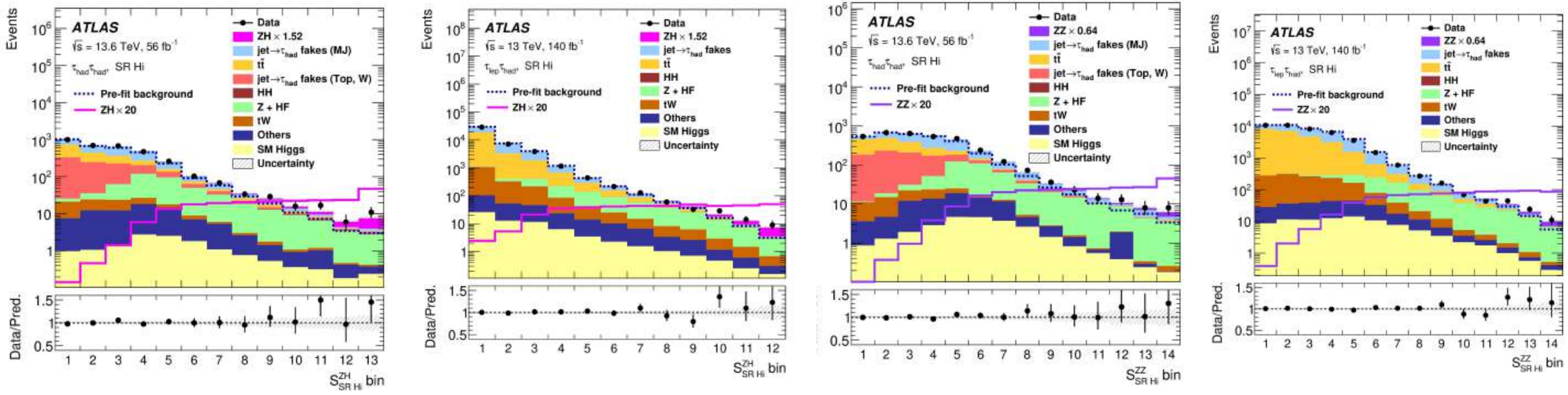

HH→bb$\tau\tau$ - CMS (Run 3 $\mathcal{L}$ =110 fb^{-1})

- Triggering primarily on leptons
- Background modelling mostly with MC + data-driven estimation of other objects faking taus
- Categorisation based on H→$\tau\tau$ and H → bb topologies
- Signal extraction using 2 dedicated DNNs: ggF and VBF

20% improvement due to Run2 lumi scaling

$$\mu = 1.1^{+1.5}_{-1.3}, \mu < 4.0(3.0)$$

Obs. (exp.) significance: 0.7 (0.8) σ

Obs. (exp.) κ_λ : [-2.5,9.5] ([-1.5,8.3])

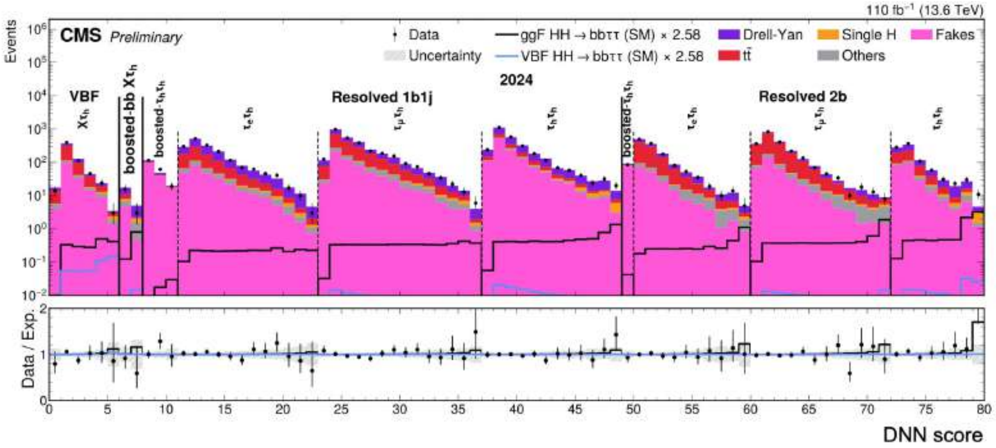

HIG-25-008 (to appear)

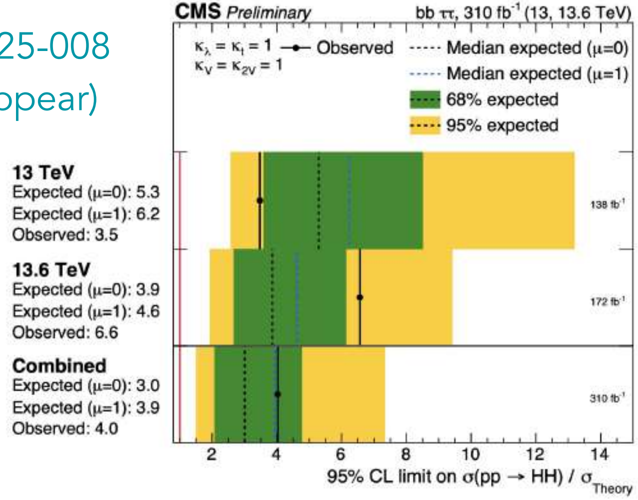

ttHH - ATLAS ($\mathscr{L}$ =140+56 fb^{-1})

- 1L: single lepton (e/μ) + ≥5 b-quarks, targeting W→ℓν and HH→bbbb decays
- SSML: ≥2 b-quarks + same-sign dilepton pair (or >2 leptons), selecting events with ≥1 leptonic W decay plus additional leptons from H→ττ/WW*/ZZ* decays
- bbγγ: ≥2 b-quarks + 2 photons, targeting HH→bbbγγ decays

SSML: Regions based on number of leptons and (b)jets

Fit transformer output

1L: Regions based on b-tag score

Fit transformer output

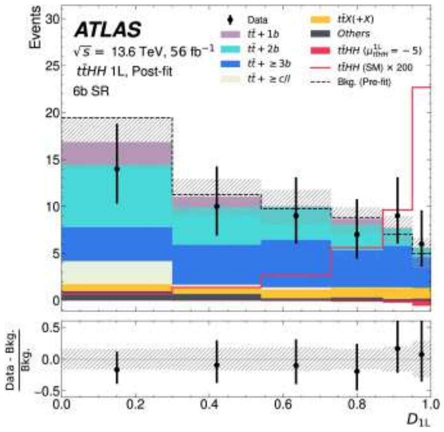

bbbγγ: Regions based on BDT cuts

Fit $m_{\gamma\gamma}$

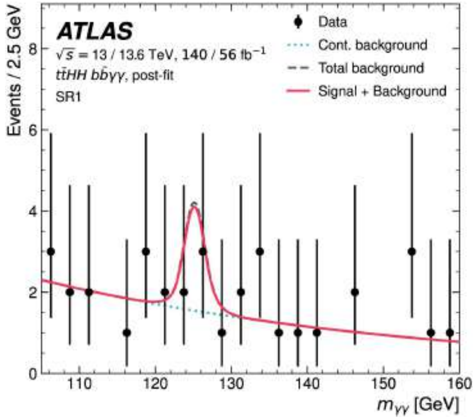

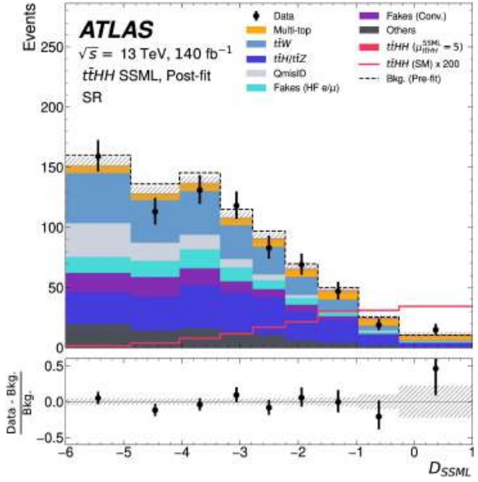

CERN-EP-2026-045

ttHH - ATLAS ($\mathscr{L}$ =140+56 fb^{-1})

- μ_{ttHH} < 20 driven by the 1ℓ channel (HH→bbbb)
- Limited by statistics and multi-top modeling

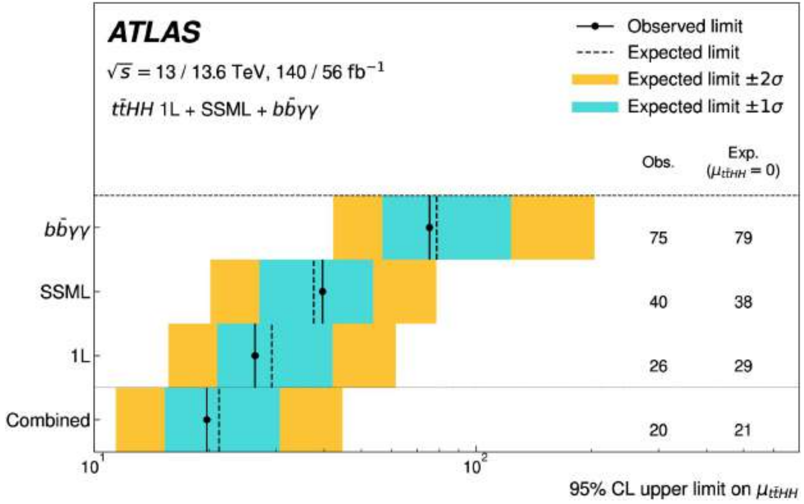

$$\mu_{t\bar{t}HH} = -3^{+11}_{-12}$$

constraints on c_{ttHH} extracted using the same phase space, multivariate discriminant, and analysis regions as the rest of the analysis

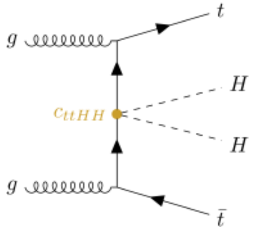

interpreted within HEFT (ttHH vertex absent in the SM, present at LO in HEFT): excludes quartic coupling outside -3.9 < c_{ttHH} < 3.3

CERN-EP-2026-045

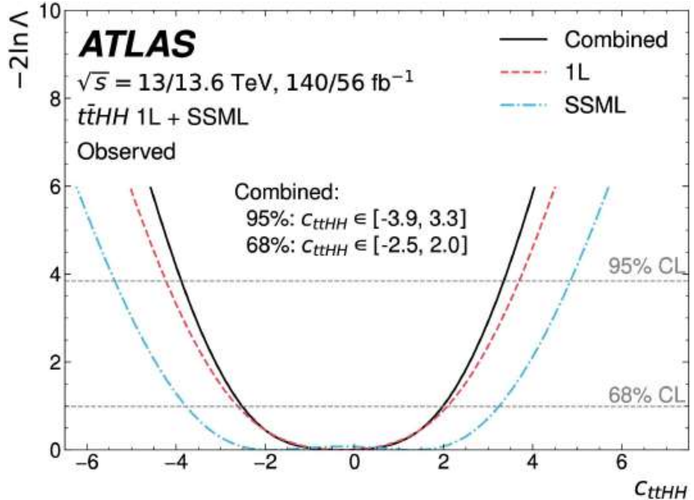

ttHH (HH → bbbb) - CMS (Run 2 $\mathcal{L}$ = 138 fb^{-1})

- Select events with 1 isolated lepton and ≥5 jets (≥4 b-tagged); topological reconstruction via a dedicated BDT (JABDT)
- DNN classifier discriminates background across 9 categories: ttHH, tt (subdivided into 4), ttH, ttZ, ttZZ & ttZH
- Signal extracted via a simultaneous binned profile-likelihood fit
- Obs (exp) 95% CL upper limit: 49 (55) × σSM, using 138 fb^{-1}

HIG-24-016 (to appear)

- Interpreted within HEFT: excludes quartic coupling outside $-6.6 < c_{ttHH} < 6.4$

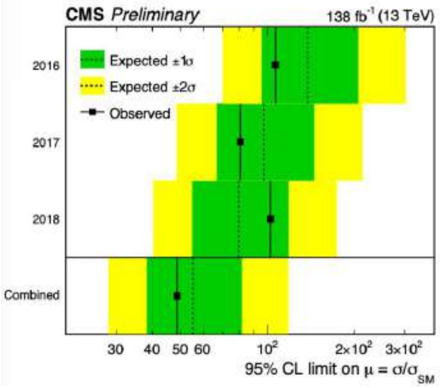

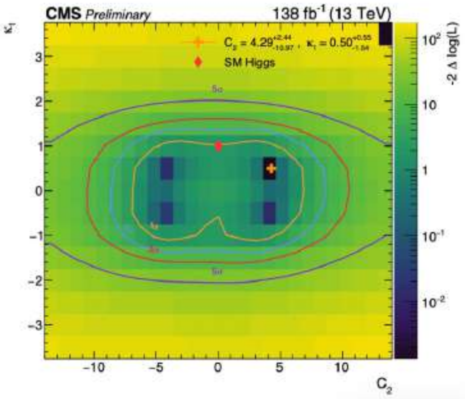

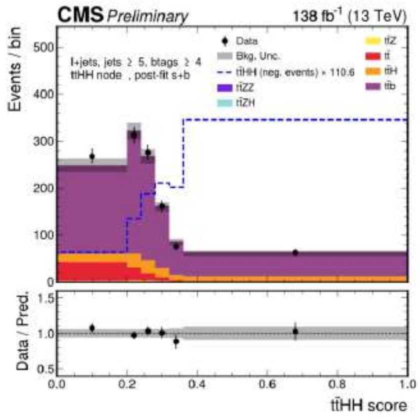

HL-LHC projections

HH sensitivities

- Improved analysis techniques (independent of detector upgrades) already yield a much stronger projection than the previous European Strategy estimate
- Continued optimization through the LHC run and HL-LHC phase is expected to push the κ_3 uncertainty well below 30%

	2 ab^{-1} (*S2*) ATLAS	2 ab^{-1} (*S2*) CMS	3 ab^{-1} (*S2*) ATLAS	3 ab^{-1} (*S2*) CMS	3 ab^{-1} (*S3*) ATLAS	3 ab^{-1} (*S3*) CMS
HH statistical significance						
$b\bar{b}\tau^+\tau^-$	$3.0^\dagger$	1.9	$3.5^\dagger$	2.4	**$3.8^\dagger$**	**2.7**
$b\bar{b}\gamma\gamma$	$2.1^\dagger$	$2.0^\dagger$	$2.4^\dagger$	$2.4^\dagger$	**$2.6^\dagger$**	**$2.6^\dagger$**
$b\bar{b}b\bar{b}$ resolved	0.9	$1.0^\dagger$	1.0	$1.2^\dagger$	**1.0**	**$1.3^\dagger$**
$b\bar{b}b\bar{b}$ boosted	–	$1.8^\dagger$	–	$2.2^\dagger$	–	**$2.2^\dagger$**
Multilepton	$0.8^\dagger$	–	$1.0^\dagger$	–	**$1.0^\dagger$**	–
$b\bar{b}\ell^+\ell^-$	$0.4^\dagger$	–	$0.5^\dagger$	–	**$0.5^\dagger$**	–
Combination	3.7	3.5	4.3	4.2	**4.5**	**4.5**
ATLAS+CMS	6.0		7.2		**7.6**	
κ_3 68% confidence interval						
$b\bar{b}\tau^+\tau^-$	$[0.3, 1.8]^\dagger$	[0.1, 3.0]	$[0.4, 1.7]^\dagger$	[0.2, 2.2]	**$[0.5, 1.6]^\dagger$**	**[0.3, 2.0]**
$b\bar{b}\gamma\gamma$	$[0.3, 2.0]^\dagger$	$[0.2, 2.3]^\dagger$	$[0.4, 1.8]^\dagger$	$[0.3, 2.0]^\dagger$	**$[0.5, 1.7]^\dagger$**	**$[0.4, 1.9]^\dagger$**
$b\bar{b}b\bar{b}$ resolved	[−0.7, 6.3]	$[-0.6, 7.6]^\dagger$	[−0.5, 6.1]	$[-0.3, 7.3]^\dagger$	**[−0.5, 6.1]**	**$[-0.3, 7.2]^\dagger$**
$b\bar{b}b\bar{b}$ boosted	–	$[-0.6, 8.5]^\dagger$	–	$[-0.4, 8.2]^\dagger$	–	**$[-0.4, 8.2]^\dagger$**
Multilepton	$[-0.2, 4.9]^\dagger$	–	$[-0.1, 4.7]^\dagger$	–	**$[-0.1, 4.7]^\dagger$**	–
$b\bar{b}\ell^+\ell^-$	$[-2.4, 9.3]^\dagger$	–	$[-2.2, 9.2]^\dagger$	–	**$[-2.1, 9.1]^\dagger$**	–
Combination	[0.6, 1.5]	[0.4, 1.7]	[0.6, 1.5]	[0.5, 1.6]	**[0.6, 1.4]**	**[0.6, 1.5]**
ATLAS+CMS uncertainty	−32% / +37%		−27% / +31%		**−26% / +29%**	

† *used in the ATLAS+CMS combination*

Combined significance above 7σ

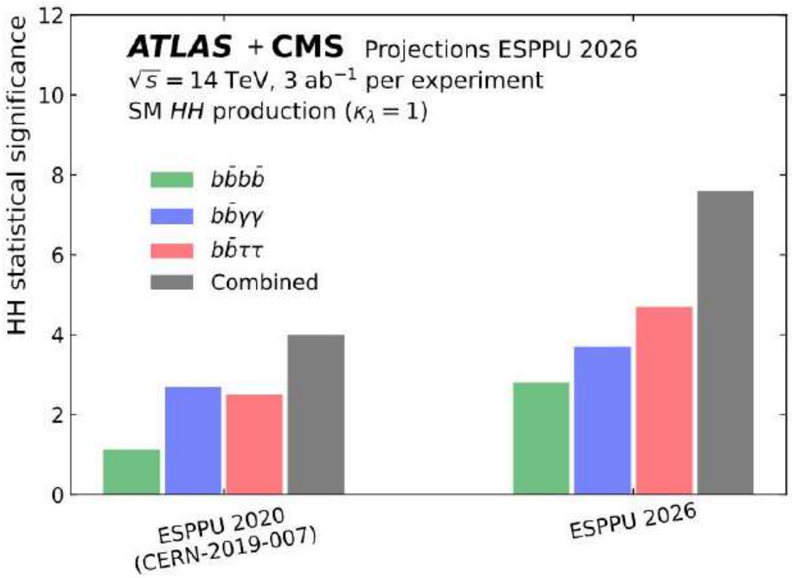

ATL-PHYS-PUB-2025-018
CMS-HIG-25-002

HH sensitivities

- κ_3 likelihood scan, S3, 3 ab^{-1}: combined ATLAS+CMS scan yields a 68% CL interval of $\kappa_3 \in [0.74, 1.29]$, consistent with a single, well-defined minimum around κ_3=1
- κ_{2V} scan, S2 vs. S3, 3 ab^{-1}: based on the boosted VBF HH→bbbb search, comparing the two systematic scenarios — S2 gives $\kappa_{2V} \in [0.87, 1.16]$ while S3 gives [0.90, 1.13], a modest but real gain from the same 5% b-tagging/τh efficiency improvements assumed in S3

ATL-PHYS-PUB-2025-018 CMS-HIG-25-002

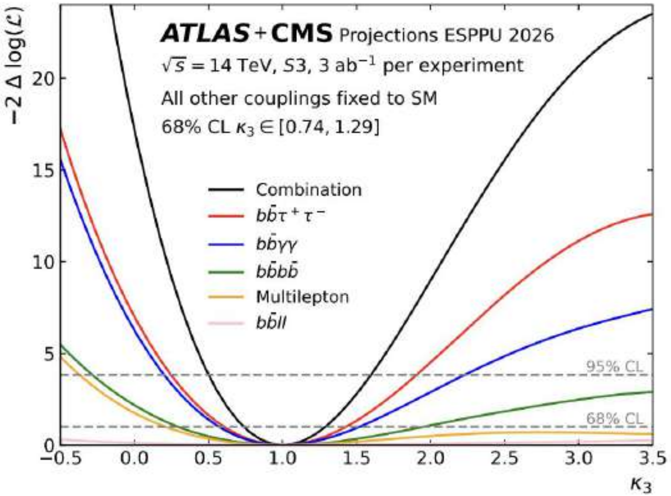

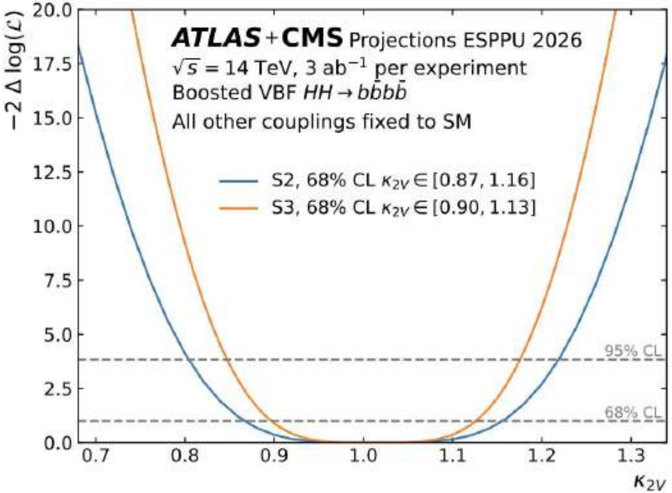

The potential shape

- SM BEH potential and the expected κ_3 precision band are compared against four alternative EWSB potentials that could still allow a strong first-order phase transition (FOPT) in the early Universe
- Arrows on each curve mark the direction of shape variation required for a strong FOPT, with parameter values as given in the legend
- Red band: model-independent, κ3-only constraint from ATLAS/CMS HH projections, valid near the minimum;
- Blue band: same constraint reinterpreted in SMEFT 6, extending validity across a much wider potential range

ATL-PHYS-PUB-2025-018
CMS-HIG-25-002

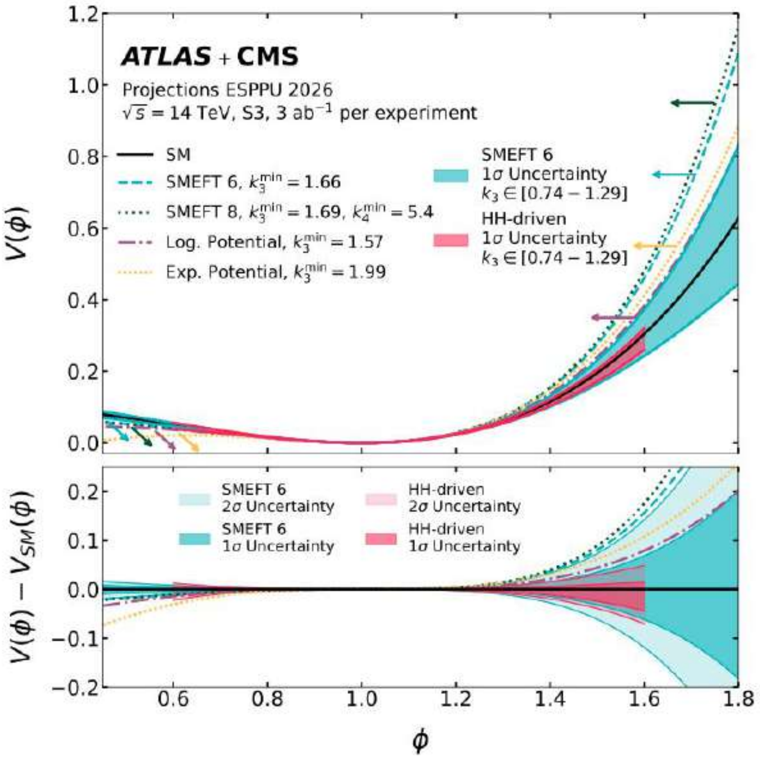

Concluding remarks

- ATLAS and CMS are exploiting the LHC's full potential in Higgs physics: mass at 0.1%, width at 40%, off-shell production confirmed, couplings at 5–10% precision, with first evidence emerging for rare production/decay modes
- ML and improved reconstruction are transforming analysis sensitivity — reshaping expectations for the Higgs self-coupling in Run 3 and making charm-Yukawa evidence at HL-LHC increasingly realistic
- ~450 fb^{-1} of Run 2+3 data still to analyze, with HL-LHC ahead — exciting chapters of Higgs physics still to come
- Highlight: detailed Higgs boson characterization and the most sensitive HH search to date ($HH \to bb\tau\tau$)

Thanks for your attention!

Additional slides

Higgs boson production per decay channel

- Measurements of $\sigma_i \times B_f$ *(floating production cross sections times BR)*
- Combining or separating production modes:
  - Driven by experimental sensitivity and ability to distinguish different process in a given decay channel
- Up to 70% improvement in total uncertainties (for WH/ZH WW)
- Good agreement between the measurements and SM predictions p_{SM} = 53%

CERN-EP-2026-228

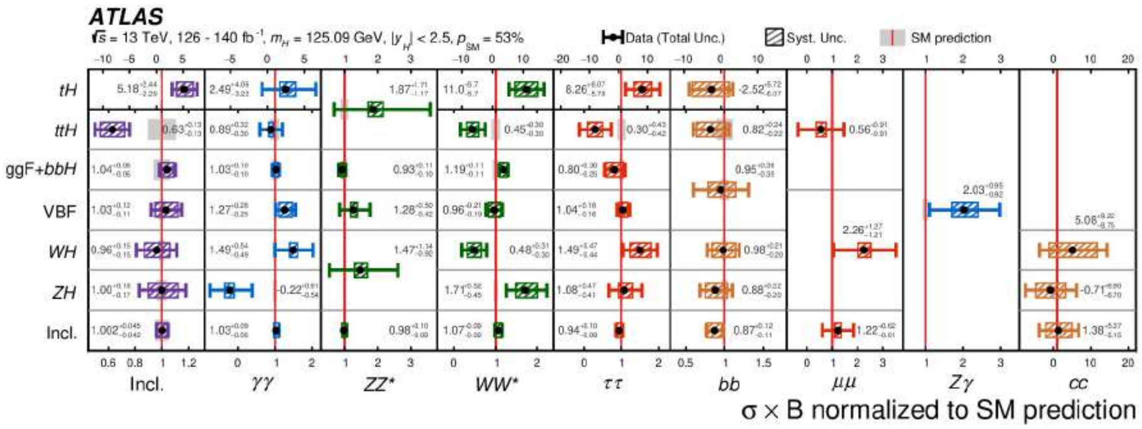

Resolved κ coupling with $B_{inv} = B_u = 0$

- Loop-induced couplings (κ_g, κ_γ, $\kappa_{Z\gamma}$) are resolved assuming no BSM decay (on-shell)
    - POIs: κ_W, κ_Z, κ_t, κ_b, κ_τ, κ_μ, (κ_c)
- Two models: $\kappa_c = \kappa_t$ and floating κ_c
    - Uncertainties of $\kappa_{Z/W/t/\tau}$ at 5%-10% level
    - Uncertainties of κ_b at 10%-15% level
    - Upper limit on κ_c of 4.1×SM at 95% CL
    - Up to 45% improvement compared to Nature combination
    - SM compatibility p_{SM} = 69% and 77%

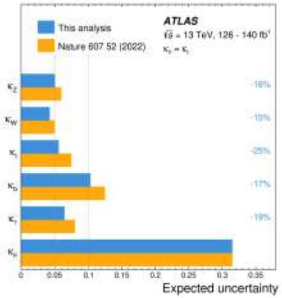

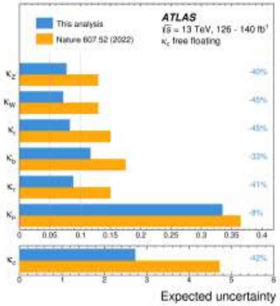

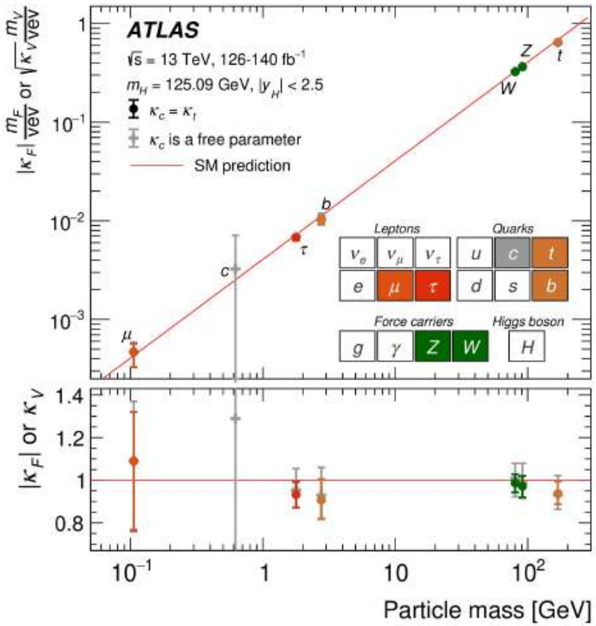

mb (mH)

- Quark masses are "running constants" in QCD due to renormalization;
  - PDG world average m_b(m_b) = 4.18 (+0.03/−0.02) GeV,
  - LEP/SLD average m_b(m_Z) = 2.82 ± 0.28 GeV
- Measurable at the LHC via H→bbb coupling: assuming SM Yukawa, the decay rate scales quadratically with m_b
- First m_b(m_H) result (ATLAS+CMS, PRL): m_b(m_H) = 2.60 (+0.36/−0.31) GeV — 1σ compatible with the SM running prediction, and differs from a no-running scenario by 7σ

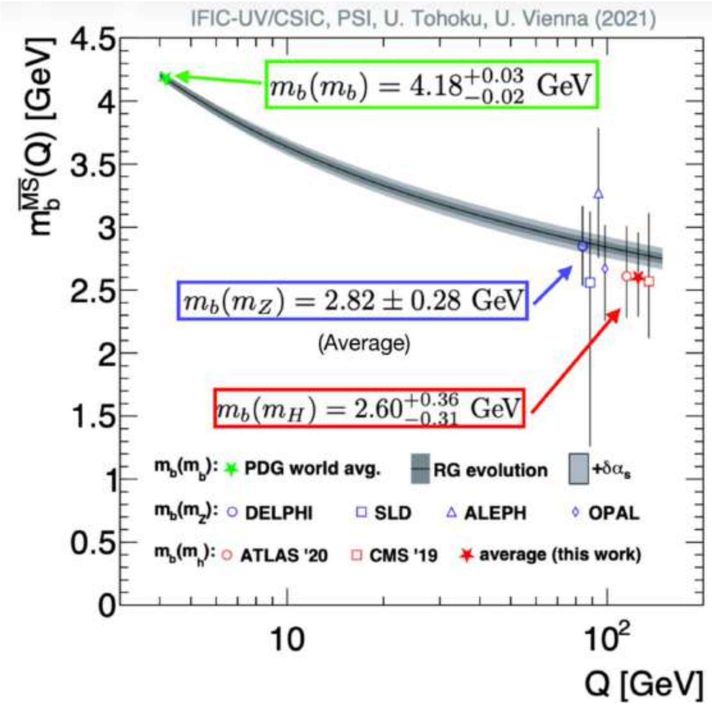

NLO EWK corrections on single Higgs

The measured production cross-section and branching fractions (BR) can be parametrized as a function of $\kappa\lambda$

- $C1$ is the process and kinematic- dependent coefficients which encodes the magnitude of the $\kappa\lambda$-dependent corrections (linear correction)
- $ZH\ BSM$ is the wave function renormalization (universal correction)
- KEW factors represents the full set of NLO EW corrections

$\sigma(\kappa_\lambda)/\sigma_{SM}$

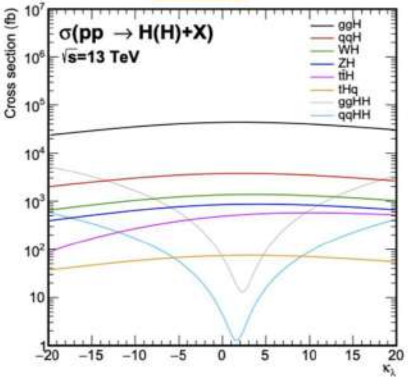

$BR(\kappa_\lambda)/BR_{SM}$

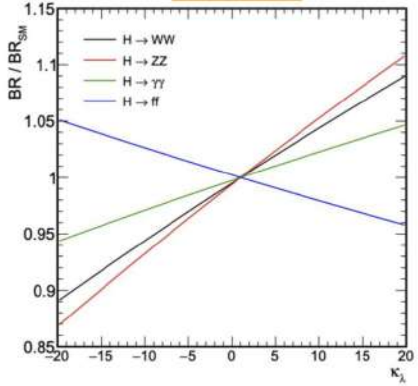

$$\mu_i(\kappa_\lambda, \kappa_i) = \frac{\sigma^{\mathrm{BSM}}}{\sigma^{\mathrm{SM}}} = Z_H^{\mathrm{BSM}}(\kappa_\lambda)\left[\kappa_i^2 + \frac{(\kappa_\lambda - 1)C_1^i}{K_{\mathrm{EW}}^i}\right]$$

$$\mu_f(\kappa_\lambda, \kappa_f) = \frac{\mathrm{BR}_f^{\mathrm{BSM}}}{\mathrm{BR}_f^{\mathrm{SM}}} = \frac{\kappa_f^2 + (\kappa_\lambda - 1)C_1^f}{\sum_j \mathrm{BR}_j^{\mathrm{SM}}\left[\kappa_j^2 + (\kappa_\lambda - 1)C_1^j\right]},$$

HH → bbγγ - ATLAS

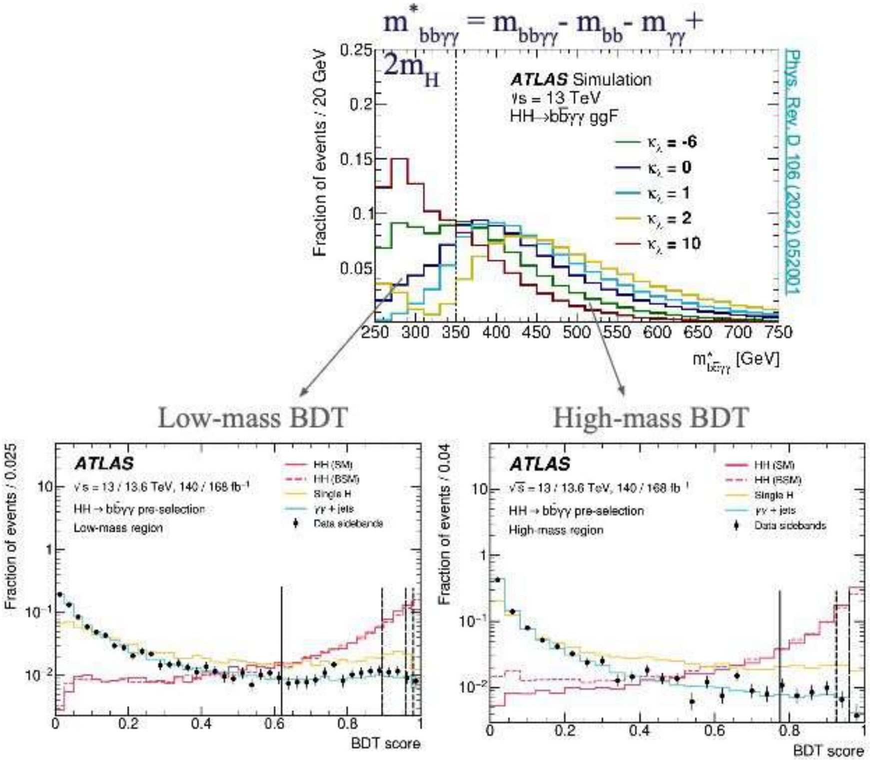

Source of systematic uncertainty	Relative impact [%] Up	Down
Experimental		
Photon energy scale	+22	−34
Photon energy resolution	+14	−7.5
Photon efficiency	+13	−2.5
Jet	+10	−6.9
Luminosity	+6.7	−1.2
Theory		
QCD scale + m_{top}, PDF+α_S	+35	−5.2
$\mathcal{B}(H \to \gamma\gamma, b\bar{b})$	+10	−2.1
Parton showering model	±15	
Heavy-flavour content	±30	
Background model		
Spurious signal	±7.2	

HH→bb$\tau\tau$ - ATLAS (140+56 fb^{-1})

Variable	Description
Global event-level features: both channels	
m_{HH}	Invariant mass of the reconstructed HH system using the di-τ four-momentum after the MMC algorithm
m_{bb}	Invariant mass of the b-jet pair
ΔR_{bb}	ΔR between the two b-jets
m_{jj}	Invariant mass of the two leading VBF jets
ΔR_{jj}	ΔR between the two leading VBF jets
$\eta_{\mathrm{VBF}\ j_0} \cdot \eta_{\mathrm{VBF}\ j_1}$	Product of pseudorapidities of the two leading VBF jets
Global event-level features: $\tau_{\mathrm{had}}\tau_{\mathrm{had}}$ only	
$\Delta R_{\tau\tau}$	ΔR between the two τ_{had} candidates
Global event-level features: $\tau_{\mathrm{lep}}\tau_{\mathrm{had}}$ only	
$\Delta R(\tau_{\mathrm{had}}, \ell)$	ΔR between the τ_{had} candidate and the electron or muon
$p_{\mathrm{T},HH}$	Transverse momentum of the reconstructed HH system
η_{HH}	Pseudorapidity of the reconstructed HH system
$E_{\mathrm{T}}^{\mathrm{miss}}$	Missing transverse energy
$\Delta R(b_0, \tau_{\mathrm{had}})$	ΔR between the leading b-jet and the τ_{had} candidate
$\Delta R(b_1, \tau_{\mathrm{had}})$	ΔR between the subleading b-jet and the τ_{had} candidate
$m_{b\ell}$	$\min(x, y)$, where $x = \max(m_{b_1,\tau_{\mathrm{had}}}, m_{b_2,\ell})$ and $y = \max(m_{b_1,\ell}, m_{b_2,\tau_{\mathrm{had}}})$
$m_{\tau\tau}^{\mathrm{vis}}$	Invariant mass of the visible di-τ system
$p_{\mathrm{T},\tau\tau}^{\mathrm{vis}}$	Transverse momentum of the visible di-τ system
T_1	Topness , with $\sigma_t = \sigma_W = 5$ GeV
H_{T}	Scalar sum of transverse momenta of all reconstructed objects
$\Delta\eta(bb, \tau\tau)$	$\Delta\eta$ between the b-jet pair and the MMC di-τ systems
$\Delta\phi(\tau\tau, E_{\mathrm{T}}^{\mathrm{miss}})$	$\Delta\phi$ between $\vec{p}_{\mathrm{T}}^{\mathrm{miss}}$ and the MMC di-τ system
$\Delta R(b_1, \ell)$	ΔR between the subleading b-jet and the lepton
$m_{\mathrm{T}}(\tau_{\mathrm{had}}, \vec{p}_{\mathrm{T}}^{\mathrm{miss}})$	Transverse mass of the τ_{had} candidate and $\vec{p}_{\mathrm{T}}^{\mathrm{miss}}$ system
Object-level features (per-object inputs to the transformer network)	
η	Pseudorapidity; set to 0 for $\vec{p}_{\mathrm{T}}^{\mathrm{miss}}$
ϕ	Azimuthal angle
m	Mass; set to 0 for $\vec{p}_{\mathrm{T}}^{\mathrm{miss}}$, leptons, and τ_{had} candidates
p_{T}	Transverse momentum
PCBT	GN2 pseudo-continuous b-tagging score (bins: 100%–90%–85%–77%–70%–65%) set to −2 for non-jet objects and −1 for forward jets
isTau	Boolean flag: object is a τ_{had} candidate
isJet	Boolean flag: object is a non-b-tagged jet
isBjet	Boolean flag: object is a b-tagged jet
isMET	Boolean flag: object is $\vec{p}_{\mathrm{T}}^{\mathrm{miss}}$
isMMC	Boolean flag: object is the MMC di-τ system
isLepton	Boolean flag: object is a lepton (only in $\tau_{\mathrm{lep}}\tau_{\mathrm{had}}$ channel)

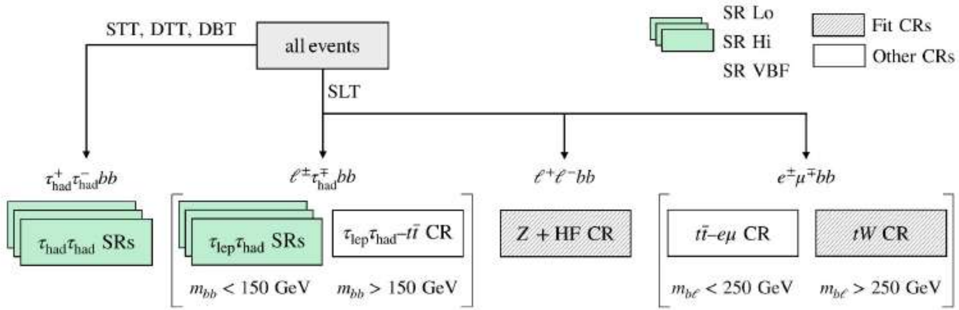

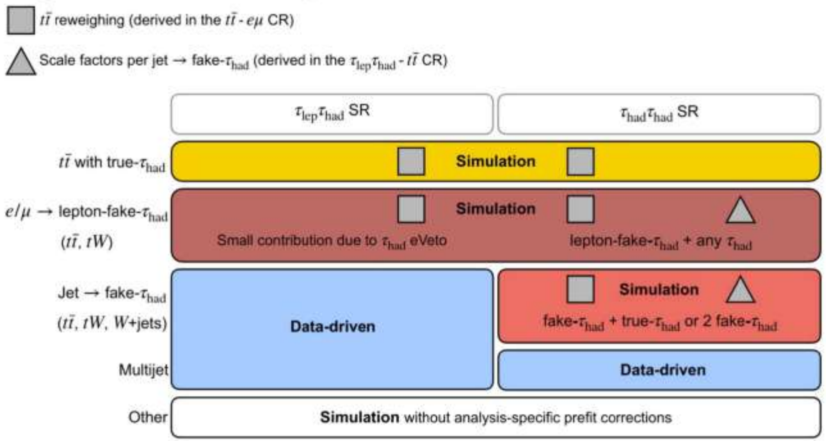

HH→bb𝛕𝛕 - ATLAS (140+56 fb^{-1})

Source of uncertainty	$\sigma_{\mu_{HH}}$
Total	1.20
Statistical	0.91
Systematic	0.76
Experimental uncertainties	0.20
Electron and muon	0.01
τ_{had}	0.13
E_T^{miss}	0.03
Jet	0.14
Flavour tagging	0.04
Pile-up	0.01
Luminosity	0.03
Modelling uncertainties	0.71
Background template statistical	0.21
HH	0.54
ZH	0.02
ZZ	<0.01
Other SM Higgs	0.25
Z+jets	0.07
tW	0.21
Top	0.12
jet → τ_{had} fakes	0.07
Others	0.01

Source of uncertainty	$\sigma_{\mu_{ZH}}$	$\sigma_{\mu_{ZZ}}$
Total	0.50	0.37
Statistical	0.39	0.28
Systematic	0.30	0.24
Experimental uncertainties	0.14	0.12
Electron and muon	0.02	0.02
τ_{had}	0.05	0.03
E_T^{miss}	0.02	0.02
Jet	0.13	0.10
Flavour tagging	0.02	0.02
Pile-up	0.01	0.01
Luminosity	0.01	0.01
Modelling uncertainties	0.26	0.21
Background template statistical	0.10	0.09
HH	0.01	<0.01
ZH	0.09	<0.01
ZZ	<0.01	0.04
Other SM Higgs	0.11	<0.01
Z+jets	0.14	0.17
tW	0.06	0.03
Top	0.07	0.05
jet → τ_{had} fakes	0.03	0.03
Others	<0.01	0.04

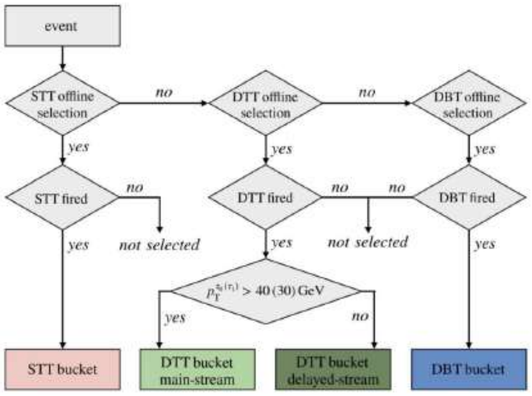

HL-LHC uncertainty source scenarios

- S2: assumes b-jet and τh identification efficiencies unchanged from Run 2
- S3: assumes a 5% improvement in both b-jet identification efficiency (at fixed light-flavour rejection) and τh identification efficiency (at fixed efficiency on hadrons)
- Both scenarios share reduced systematic uncertainties vs. Run 2: statistical-origin systematics shrink toward "floor" values with luminosity, theory uncertainties are halved, MC statistical uncertainties are treated as negligible (thanks to ML-based large-sample generation), and data-driven background uncertainties scale down with √(luminosity increase)

Table 3: Reduction of the systematic uncertainties common to several input channels

Uncertainty	Reduction with respect to Run 2
Luminosity	0.6
bjet tagging efficiency	0.5
cjet tagging efficiency	0.5
Light-jet tagging efficiency	1
Jet energy scale and resolution	1
Photon efficiency	0.5
Photon energy scale and resolution	1
τ_h efficiency (statistical components)	Not considered
τ_h efficiency (systematic components)	1.0
τ_h energy scale	1.0
τ_h misidentification efficiency	1.0
Statistical uncertainties of Montecarlo samples	Not considered
Theoretical uncertainties	0.5

Uncertainty source	Uncertainty scale factor		
	Run 2 systematic uncertainties	Baseline	No systematic uncertainties
Background modelling uncertainties	1.0	0.0	0.0
MC statistical uncertainties	1.0	0.0	0.0
Photon identification and isolation	1.0	0.8	0.0
Flavour tagging of b, c jets	1.0	0.5	0.0
Other experimental systematic uncertainties	1.0	1.0	0.0
Theoretical uncertainties	1.0	0.5	0.0